Specimen Size Effects In Slow Strain-Rate Testing

by

William C. Porr, Jr.

Thesis submitted to the Faculty of the

Virginia Polytechnic Institute and State University

in partial fulfillment of the requirements for the degree of

Master of Science

in

Materials Engineering

APPROVED:

M. R. Louthan, Jr., Chairman

R. W. Hendricks

N. E. Dowling

August 25, 1987

Blacksburg, Virginia

Specimen Size Effects In Slow Strain-Rate Testing

by

William C. Porr, Jr.

M. R. Louthan, Jr., Chairman

Materials Engineering

(ABSTRACT)

A study was conducted to evaluate the effect of specimen dimensions in slow strain-rate environmental effects testing. Tension tests of free machining brass were conducted in a mercuric nitrate solution at a constant crosshead displacement rate of $10^{-3}\frac{inch}{sec}$. Thirty-six smooth round bar specimens with different dimensions were tested. It was shown that percent elongation to failure was inversely proportional to an effective ratio of length to diameter, $\frac{(D-2a)L}{D^2}$, where D is the specimen diamter, L is the length of the reduced cross section of the specimen, and a is the environmentally induced crack depth. This effective length to diameter ratio correlates with the applied tearing modulus for a cracked round bar tension specimen as defined by P. C. Paris and co-workers in 1979. The results verify that the tearing modulus may be used as a parameter to evaluate tearing instability in terms of elastic-plastic fracture mechanics. More directly, these results show a possible source of error in evaluating the degree of susceptibility to environmentally induced cracking in a material-environment interaction.

Acknowledgements

I would like to express my sincerest gratitude to my advisor, Dr. M. R. Louthan, Jr., for his guidance not only in my research work and education, but in my life as well. He has shaped my future in more ways than I'm sure we realize. I greet his imminent return to industry with mixed emotions: Happiness that he and his family will truly be happy, yet sadness that the educational community is losing a tremendous teacher. If feel lucky I caught him before he left.

I would also like to express my gratitude to Dr. R. W. Hendricks and Dr. N. E. Dowling for their input to this thesis. Thanks also goes to Dr. R. E. Swanson for his willingness to help in the area of stress-corrosion cracking.

It is important to realize that the people that contributed to my education did not all have PhD.'s. Thanks are necessary to those co-workers and friends that made my life at Virginia Tech enjoyable: , friend and mom away from home; my idol in the art of procrastination; the multitalented ; office mates ; fellow NASCAR fan ; my running buddies ; and of course, the entire staff of the Ton-80 club. It would be impossible to forget the women of my life, namely the secretaries of Materials Engineering: and especially whose patience and typing wizardry made this thesis readable.

Special thanks to those close friends that will always command my respect: who has been there forever; , always unflappable and rarely too concerned about anything; , a man of a thousand words - a year; and , the closest thing to a brother I've ever had, ugly as he is.

More than thanks and respect are necessary to those who truly are responsible for any success I may ever have. My parents, my sisters, and my grandmother deserve my love along with my thanks and respect.

These people, all of them, did the hard work. I just took the classes and wrote the thesis.

Table of Contents

List of Illustrations

List of Tables

1.0 Introduction

The problem of stress-corrosion cracking, the combined failure process of tensile stress and environment, has long been recognized by engineers. As a result, test methods have been developed to analyze, assess, and evaluate stress corrosion tendencies in many different alloy-environment combinations. Attempts are made to duplicate possible in-service conditions with simple tests. Common testing in the past has involved a constant load apparatus where time-to-failure was the measured paramater. This type of testing, although effective, was very time consuming. In the past two decades, slow strain rate testing has been widely adopted to determine stress-corrosion cracking (SCC) tendencies in materials.

Slow strain-rate testing (SSRT) is normally conducted by loading a sample in tension using a constant strain-rate while the specimen is in a specified environment. Measured parameters to evaluate SCC tendencies include elongation to failure, reduction in area, time to failure, crack growth, crack velocity, and stress intensity. The last of these is significant because it represents the inclusion of linear elastic fracture mechanics (LEFM) in the SCC evaluation.

About the same time SSRT was gaining acceptance, elastic-plastic fracture mechanics (EPFM) in terms of the J-integral was becoming more popular among the fracture theorists. The experimental work described in this thesis centered on determining if EPFM has a significant effect on results

from slow strain-rate testing. More specifically, the question of whether elastic-plastic tearing instability affects data from slow strain-rate testing is examined.

2.0 Literature Review

2.1 Slow Stain-Rate Testing

Slow strain-rate testing provides a rapid laboratory test to evaluate stress corrosion cracking in a material-environment combination. This test method will show SCC susceptibility not generally seen in constant load or constant deflection tests. J.H. Payer and co-workers describe the slow strain-rate test as "positive" because failure ultimately occurs in either a ductile manner or prematurely due to environmental cracking [1, 2].

Development of the slow strain-rate test for SCC studies began in Great Britain in the mid 1960's under the leadership of R.N. Parkins, who has described the history and techniques of slow strain-rate testing in several publications [3, 4, 5]. Both he and Payer place rather flexible requirements on test techniques. They describe the test method as involving plain tensile specimens strained at a constant rate in a relatively stiff- framed test machine [1, 2, 3, 4, 5]. The strain rate must be carefully selected to allow for the environmental effects to occur. If the rate is too fast, ductile fracture will occur and the test results will be inconclusive.

With these minimal test procedure requirements, it is easy to vary test conditions to determine the effects of many variables. The complexity of the variations is evident in examples such as the effect of crosshead speed and temperature in SCC of α-brass in an ammoniacal solution [6], the effects of crosshead speed, solution chemistry changes, ammonia content, solution pH, anion additions, prexposure, and corrosion potential on the SCC of α-brass in ammoniacal solutions [7], and the effect of gaseous atmospheres and temperature on several different austenitic and ferritic metals [8]. Test specimen geometries that have been used in slow strain-rate testing are numerous and varied, and include single edge notch [7], notched rod [5], cracked plate [6], rectangular bar [9], square cross section [10], wire [10, 11], and round bar [10, 12]. Not only do geometries vary, but specimen dimensions in the different geometries vary as well. The most commonly used test specimen geometry is the round bar.

The American Society for Testing and Materials is the organization that sets the testing standards for most imaginable methods and materials in the United States. ASTM Standard G-49 is for the "Preparation and Use of Direct Tension Stress-Corrosion Test Specimens" and covers procedures for investigating susceptibility to stress-corrosion cracking [13]. It is stated in this specification that "axially loaded tension specimens provide one of the most versatile methods of performing a stress-corrosion test because of flexibility permitted in the choice of type and size of test specimen..." Investigators are then referenced to ASTM Standard E8 for dimensions of standard test specimens [14]. However, this requirement is not strict. The statement of this requirement begins with "whenever possible,...", and goes on to state that product dimensions determine test specimen sizes. The only warnings given for sample sizing are with regard to specimen cross section and small samples. Stress-corrosion test results are said to vary with specimen cross section, and the use of small samples below 0.4 inch gauge length or 0.12 inch in diameter are discouraged due to difficulty in machining and testing. The only stringent requirement in specimen dimensions is that the dimensions must be recorded in the reporting of results.

Once specimens are selected and tested, evaluation of the slow strain-rate test data becomes a multiple choice exercise. Treseder [15] listed a comprehensive table of possible parameters which

may be used to evaluate stress-corrosion cracking. Those that have significance to slow strain-rate testing and have been recorded in the past include crack velocity [6, 7], ultimate tensile strength [6, 7, 10, 12], time to failure [7], elongation to failure [6, 7, 8, 9, 10, 11], crack length [6], work to failure or ductility [10, 12, 16], reduction in area [8, 10, 12, 16], hardness through cross section [10, 16], and flaw SCC area [9, 10]. ASTM Standard G-49 suggests that ultimate tensile strength, elongation, or reduction of area, along with metallographic examination, be used to evaluate SCC in slow strain-rate tests. All three of these parameters are readily measurable, the elongation and UTS coming directly from a load-displacement curve. In an overview of publications on slow strain-rate testing of SCC susceptibility, it is quite apparent that these three are the most commonly reported parameters.

2.2 *Stress Corrosion Cracking and Fracture Mechanics*

For many years Engineering Mechanics specialists have been studying the effect of internal flaws or cracks on crack growth in engineering materials. Some of this fracture mechanics technology has been applied to stress-corrosion studies. It has become apparent that environmental effects and fracture mechanics can be synergistic in their roles in material failure. Much of the study in this area has concerned the plane-strain fracture toughness, K_{Iscc}. However, as late as 1984, Wei and Novak have reported that refinement in test methods and analysis is needed because of significant variation in K_{Iscc} values between testing laboratories and even within a laboratory [17]. Plane strain fracture toughness is based on linear elastic fracture mechanics (LEFM), but in ductile materials, especially for small specimens, fracture is better described by elastic-plastic fracture mechanics (EPFM). For this reason, the application of EPFM to SCC studies is beginning to appear more frequently in the literature [18, 19, 20].

2.3 *The J-Integral*

Prior to 1968, fracture mechanics was based upon linear elastic behavior of materials. The theory in crack tip stress analysis was elastic. In 1968, J. R. Rice introduced a new elastic-plastic parameter to characterize conditions at a notch or crack [21]. He proposed J as a line integral of the form

$$J = \int_{\Gamma}(Wdy - T\frac{\partial u}{\partial x}ds) \tag{1}$$

where

x,y = Cartesian coordinates in the two-dimensional deformation field

W = strain energy density = $\int\sigma_{ij}d\varepsilon_{ij}$ where $\sigma_{ij},\varepsilon_{ij}$ are stress and strain tensors respectively

Γ = Contour around the crack tip

T = stress vector normal to Γ

u = displacement vector

ds = element of arc length on Γ

Rice went on to prove that this integral is independent of path Γ. This is important because it allows evaluation of the integral along any convenient path, such as specimen boundaries. The J-integral characterizes near crack tip behavior with respect to elastic or elastic-plastic conditions.

In 1973, Landes and Begley proposed a test procedure for establishing the onset of crack growth based on the J-integral [22]. This procedure proved valuable in establishing a critical J value for the onset of crack growth, J_{Ic}. In earlier work by the authors, J had been determined by the rate of change of the area under the load-displacement curve with crack length [23].

$$J = -\frac{1}{B}\frac{dU}{da} \tag{2a}$$

Where B is the specimen thickness in a bend test. Later [24], some convenient approximations were developed, such as the following for bend or compact specimens.

$$J = \frac{2A}{bB} \tag{2b}$$

Where b is the length of the remaining uncracked ligament, and A is the area under the load-displacement curve.

The test procedure involved loading different specimens to different displacements, taking the areas under the load displacement curves and measuring the crack extension. From this data a J - Δa plot was produced where Δa is crack extension. J_{Ic} was considered to be at the point where this plot and a "blunting line" intersected. The blunting line refers to displacement of the crack tip relative to its position to loading as caused by crack tip stretch. Landes and Begley estimated this line on the J - Δa plot as half the crack opening stretch

$$J = 2\sigma_o \Delta a \tag{3}$$

where σ_0 = yield stress

This procedure was appropriate for multiple specimen determinations of J_{Ic} and was also modified for single specimen J_{Ic} determinations. The present day ASTM specification for determining J_{Ic}, Standard E813, still uses the Landes and Begley blunting line to determine J_{Ic} [25].

2.4 *Tearing Instability*

In 1979, Paris and some fellow workers presented an analysis for unstable ductile crack growth in terms of J - Δa analysis (J-R curves) [26]. It was based on global conditions in a specimen or component that act as a driving force for unstable tearing. His derivation of a "tearing modulus," T, is most easily understood by considering a center-cracked plate of thickness, B, width, W, length, L, and crack length, 2a. The load at which net section plastic behavior would begin is given by

$$P_L = \sigma_0(W - 2a)B \tag{4}$$

where σ_0 is the yield stress. In a controlled displacement test, if plastic deformation is localized to the crack region, the crack opening stretch would equal the change in overall sample length, ΔL. Therefore

$$d(\Delta L) = d(\delta_t) \tag{5}$$

where δ_t is the crack opening stretch. In discussing crack blunting in J testing, it has already been determined that

$$\delta_t = \frac{J}{\sigma_0} \tag{6a}$$

or

$$d(\delta_t) = \frac{dJ}{\sigma_0} \tag{6b}$$

Combining equations (5) and (6b),

$$d(\Delta L) = \frac{dJ}{\sigma_0} \tag{7}$$

Now, as crack growth occurs beyond J_{Ic}, the load in equation (4) would be expected to decrease with crack growth as,

$$dP = -2\sigma_0 B da \tag{8}$$

This drop in load would be expected to allow an elastic relaxation based on Hooke's law,

$$\frac{\Delta L}{L} = \frac{\sigma}{E} \tag{9a}$$

or

$$\Delta L = \frac{\Delta P L}{AE} \tag{9b}$$

where A is the net cross sectional area.

Incrementally,

$$d(\Delta L) = \frac{dPL}{AE} = \frac{-2\sigma_0 daL}{WE} \tag{10}$$

Instability would occur when this elastic shortening equaled or exceeded the lengthening due to plastic crack opening stretch given by equation (7). Therefore, the criterion for tearing instability is given by

$$\frac{dJ}{\sigma_0} \leq 2\sigma_0 \frac{daL}{WE} \tag{11}$$

Rewriting this in terms of materials constants and specimen dimensions,

$$\frac{dJ}{da} \times \frac{E}{\sigma_0^2} \leq \frac{2L}{W} \tag{12}$$

The left side of this inequality is made up of measureable materials constants and is called $T_{material}$. The right side of this inequality is referred to as $T_{applied}$ and is based on specimen dimensions. Therefore, generically

$$T_{mat} \leq T_{app} \tag{13}$$

is the criterion for tearing instability. Paris and co-workers developed instability criterion for several different geometries including the following for a notched round bar,

$$T_{mat} \leq \frac{\sigma_f}{\sigma_0} \times \frac{4Ld}{D^2} \tag{14}$$

where variables are as previously defined and

L = specimen length

d = minor diameter

D = major diameter

σ_f = flow stress

Paris and co-workers followed this analysis of tearing instability with another publication detailing the experimental investigation of their theory [27]. By varying the length and crack size to specimen depth ratio of a 3 point bend specimen they were able to vary the applied tearing factor, T_{app}. They found very good agreement between actual physical behavior and theory. When $T_{mat} \cong T_{app}$,some marginal stability was observed, but as in any early work, unknown variables may affect the results. Recommendations for additional testing and analysis to explore other variables and specimen geometrics were included at the end of the paper. During the past eight years additional analysis and verification of the tearing instability theory of Paris and co-workers has been published [28-36]. Attempts to use the analysis for practical engineering applications has been complicated but moderately successful to this point [32, 34, 35, 37]. The research reported in this thesis centers around elastic-plastic tearing instability affecting the analysis of slow strain-rate stress-corrosion cracking data obtained from round bar tensile specimens.

3.0 Methods and Materials

The concept involved with the study described in this thesis was to run a slow strain-rate stress-corrosion cracking type study but to evaluate the data in terms of tearing instability. This meant keeping all variables constant with the exception of specimen dimensions. Specimen dimensions were varied to change T_{app}. In 1981, Prabhat and Donovan showed that the difference between stable and unstable crack growth in a double edge notched specimen was very distinguishable based on elongation to failure [36]. Since this is a commonly used parameter for analysis in SCC studies, it was considered an excellent choice for analysis in this study.

3.1 Material and Environment

Since stress-corrosion cracking was not the true subject of this study, the material-environment combination was selected to insure that cracking occurred quickly. In fact the cracking mechanism selected was liquid metal embrittlement (LME) and not SCC. However the macroscopic effect is the same, and LME sufficed in meeting the cracking needs of this study.

Free machining brass was selected as the test alloy because it is very susceptible to LME in mercury. Free machining brass is an α-brass of approximate composition 61.5% copper, 35.5% zinc, and 3% lead. A typical microstructure of this material is shown in Figure 1. Room temperature mechanical properties of the as-recieved material are listed in Table 1.

The environment for cracking was a .05m solution of mercuric nitrate. Mercury plated out of solution onto the exposed brass surface and mercury LME proceeded.

3.2 Specimen Preparation

The as-received material was in the form of six foot long round bars, ½ inch in diameter. From this, thirty-six rod tensile specimens of different dimensions were machined so that T_{app} could be varied based on the derivation by Paris and co-workers for a notched round bar. Specimens were machined to four different diameters and nine different reduced length to diameter ($\frac{L}{D}$) ratios. Figure 2 shows the specimen geometry and Table 2 shows the grid of reduced lengths and diameters for the thirty-six specimens.

After machining, all samples were surface coated with a clear acrylic except for a masked off surface area of approximately 0.21 square inches. This was done so that environmental effects took place to the same extent in each sample and to insure that any changes in elongation were not due to a different area of cracking. This also allowed for the fracture to be restricted to a specific area of the specimen.

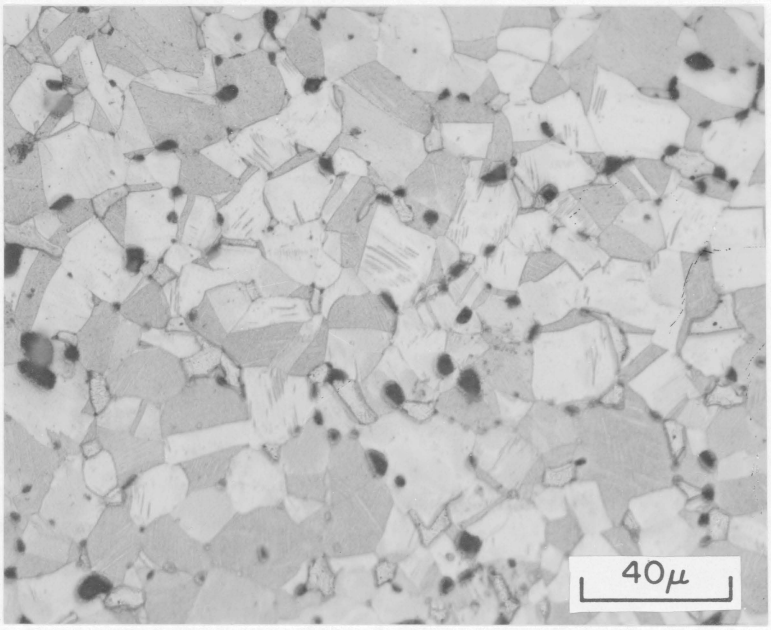

Figure 1. Microstructure of Free Machining Brass.

Table 1. Mechanical Properties

Mechanical Properties* of As-Received Free Machining Brass

Ultimate Strength	65.7 ksi
Percent Elongation to Failure	6.5
Percent Reduction in Area	30.8

*Based on an average of five tests using specimens of 0.2 inch diameter and 2.0 inch reduced section length.

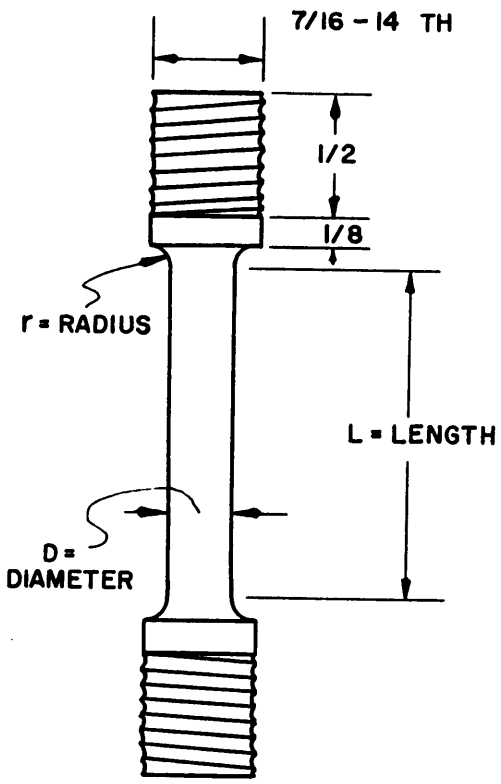

Figure 2. Tensile specimen geometry.

Table 2. Dimensions of Tension Specimens

Length to Diameter Ratio ($\frac{L}{D}$)	Length of Specimen Reduced Section, L (in)			
	Diameter = 0.15 in	Diameter = 0.20 in	Diameter = 0.25 in	Diameter = 0.30 in
3	0.45	0.60	0.75	0.90
5	0.75	1.00	1.25	1.50
6	0.90	1.20	1.50	1.80
7	1.05	1.40	1.75	2.10
10	1.50	2.00	2.50	3.00
12	1.80	2.40	3.00	3.60
15	2.25	3.00	3.75	4.50
17	2.55	3.40	4.25	5.10
20	3.00	4.00	5.00	6.00

3.3 Test Equipment

All tensile testing was done on a 22 kip capacity servohydraulic test system. The specific system was a MTS model 810 Materials Test System with a 448.82 Test Controller and a Digital PDP-11 computer. A computer program was written to conduct the test and record data using MTS BASIC software. This program is printed in Appendix A along with an example of a results printout.

A containment vessel was placed around the lower grip and specimen to hold the liquid environment as shown in Figure 3.

3.4 Test Procedure

Each specimen was placed in the testing machine and surrounded by the mercuric nitrate solution. The specimen was then pulled to failure at a constant cross-head displacement of 0.001 in/sec. Load and displacement data were collected and converted to engineering stress and percent elongation respectively by the online computer data acquisition system. These data were then plotted and printed. An example of this printout is found in Appendix A.

Optical and scanning election microscopy methods where used to examine the fracture surfaces. Crack lengths for all samples were estimated using optical microscopy. Selected samples were examined for crack path and crack morphology.

Final diameter measurements were made with Vernier calipers to an accuracy of 0.001 inches. A reduction in area was then calculated for each specimen.

Elongation was plotted as a function of T_{app} to examine the effect of specimen dimensions.

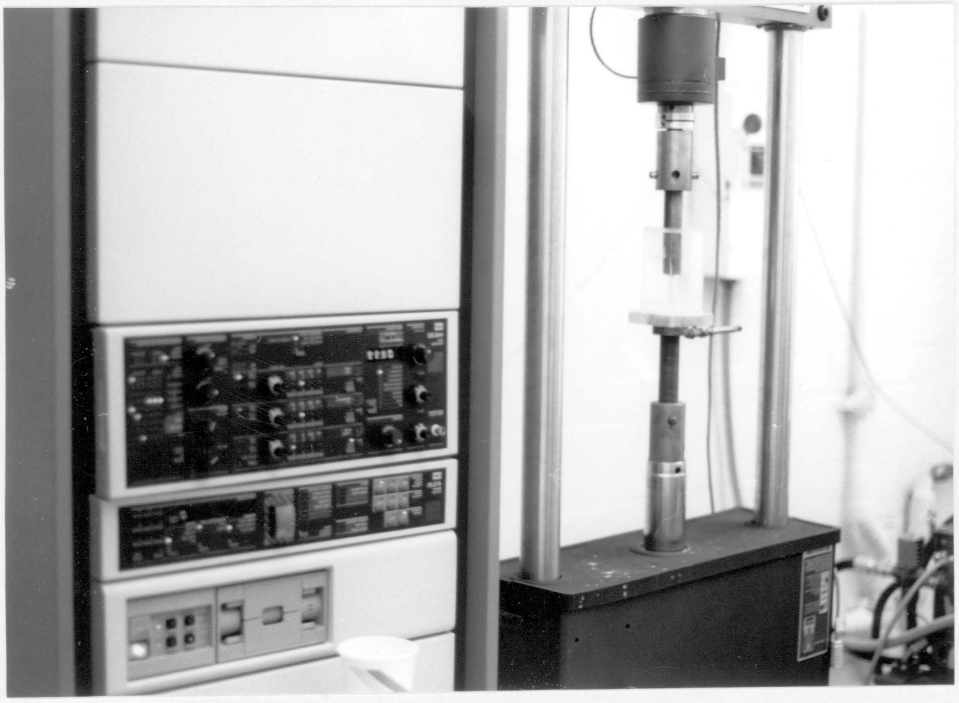

Figure 3. **Experimental set-up with MTS model 810 Materials Test System** and environmental containment vessel.

4.0 Results and Discussion

4.1 Environmental Cracking

In a slow strain-rate environmental effects test, a consistant chronology of events would be expected in the fracture process. Figure 4 shows this chronology schematically. Considering a round bar tensile specimen, as used in this study, initially it will be in an as-machined state. As it is strained, some environmentally assisted cracking will begin on the surface. In the absence of a notch to localize cracking, multiple cracking will occur over the exposed surface of the metal. With increasing strain and time, these cracks would grow radially and deeper. Ideally, one or more of these cracks would become totally annular, lending to a straightforward mechanics analysis. Eventually some critical fracture parameter would be reached and unstable crack growth and fracture would occur. The fracture parameter determining when rapid fracture occurs is either K_{Ie} or J_{Ie} . J_{Ie} determines the onset of stable crack growth in a material unless $T_{app} > T_{mat}$. If this condition exists, cracking is unstable. If $T_{mat} > T_{app}$, it might be expected that K_{Ie} determines unstable crack growth.

Figure 5 shows a picture of one of the specimen fracture surfaces. An annular ring is present showing the region of the environmentally induced crack. Figures 6 and 7 are close up pictures of

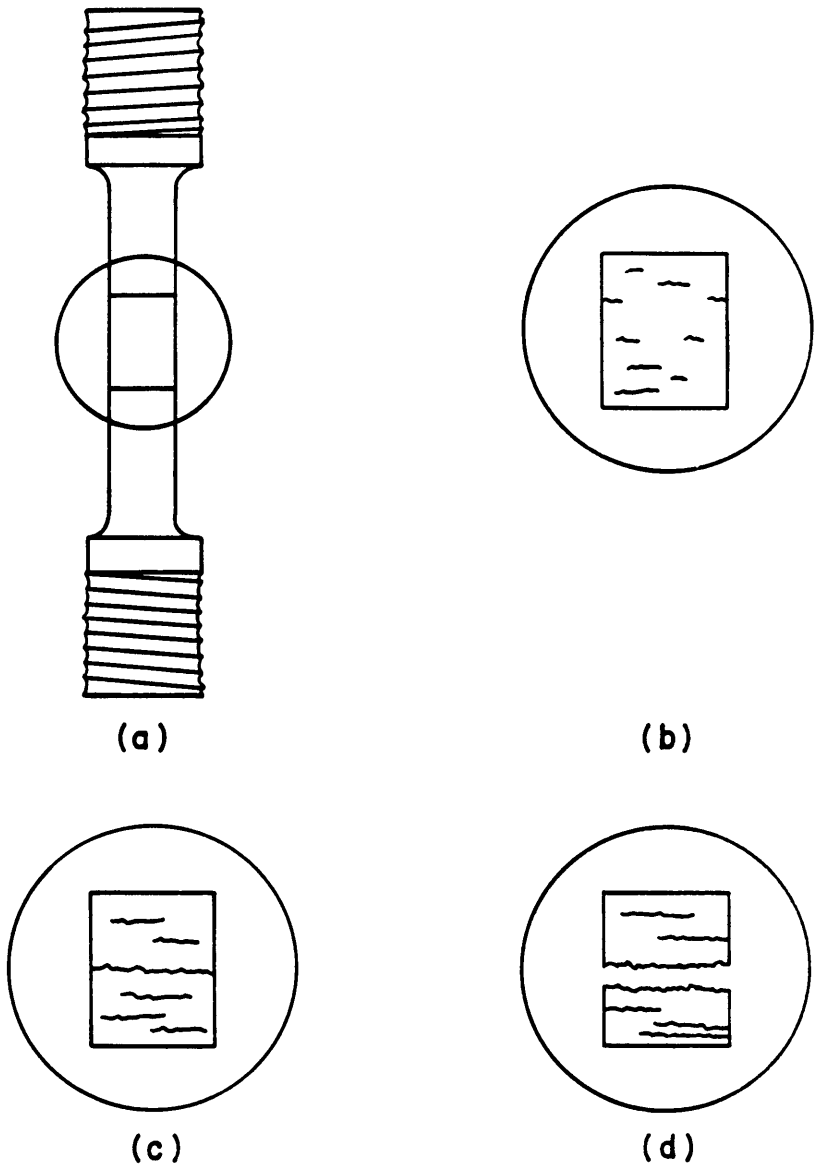

Figure 4. Schematic of expected crack growth chronology in fracture process. (a) Specimen at start of test (b) enlarged view of exposed region of speciment with cracks beginning to grow perpendicular to axis of loading as test proceeds, (c) with increasing time and strain, crack grow radially, (d) finally, a crack will become annular and final fracture occurs on the plane of this crack, perpendicular to axis of loading.

this surface. Figure 6 shows the transition region from environmentally induced intergranular fracture to ductile microvoid rupture. Figure 7 is a picture of the intergranular fracture caused by the mercury liquid metal embrittlement. This series of pictures shows that the cracking and fracture chronology described above was applicable in this case.

If an annular crack forms in a round bar test specimen, the Paris derivation for T_{app} of a notched round bar would apply. The crack would act as a very sharp notch of depth "a". This would change equation 14 to

$$T_{app} = 4(D - 2a)\frac{L}{D^2} \tag{15}$$

where the variables are the same as previously defined and $\sigma_f = \sigma_0$ assuming elastic perfectly plastic behavior. The analysis in this study assumed annular cracking. This in fact was not always the case; however, the analysis that follows was relatively unaffected. If this had not been the case; a better analysis would be one similar to that of Pan and co-workers where tearing instability was evaluated with respect to a circumferentially cracked pipe subtending an angle of 2θ [32].

4.2 Mechanical Testing

Thirty-six slow strain-rate tension tests were conducted at a constant crosshead displacement of 10^{-3} inch/sec. Data for twelve of these tests were discarded due to fault in the test procedure or fracture in a region other than that exposed to the test environment. Data for the twenty-four tests believed to be reliable are given in Tables 3 and 4. Each specimen was assigned a two digit identification number. The first digit represented the diameter of the specimen where 1 = 0.15 inch,

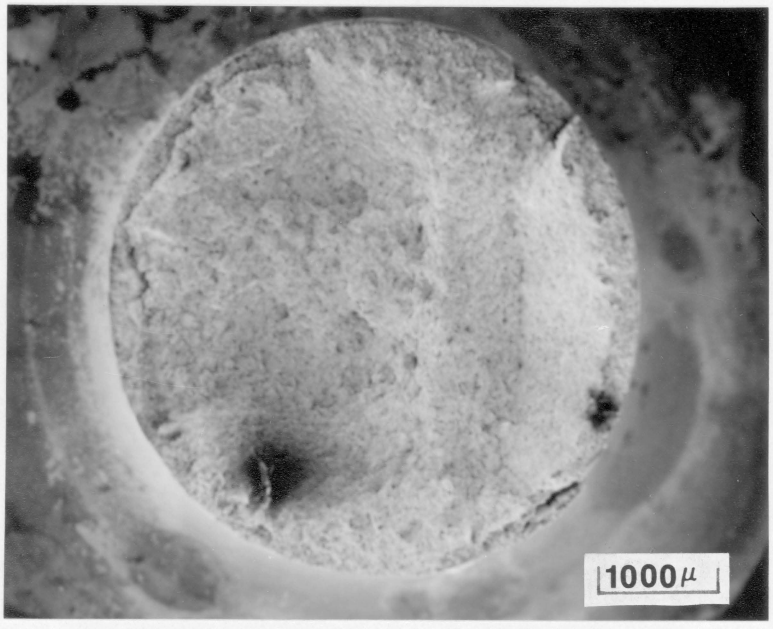

Figure 5. Fractograph of specimen 19 showing annular crack.

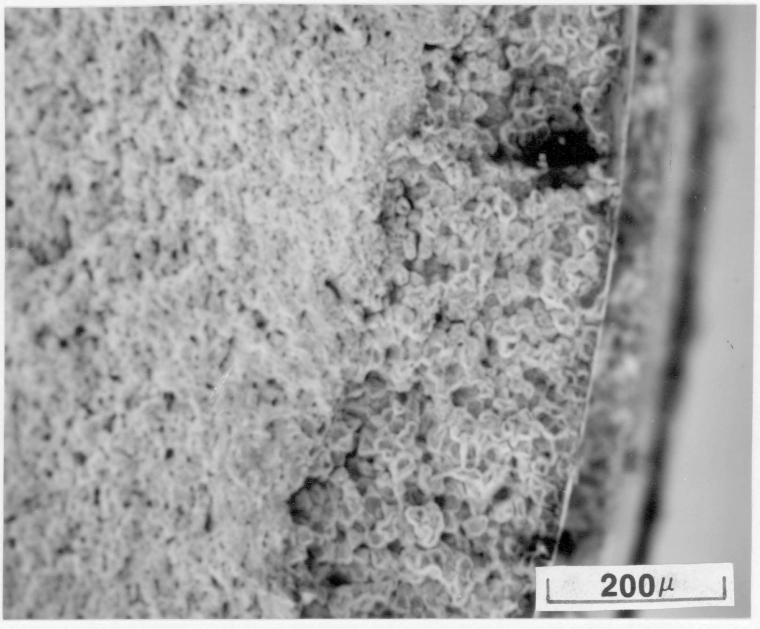

Figure 6. Fractograph of specimen 19 showing crack mode transition. Definition between intergranular, environmentally induced crack and ductile, microvoid rupture.

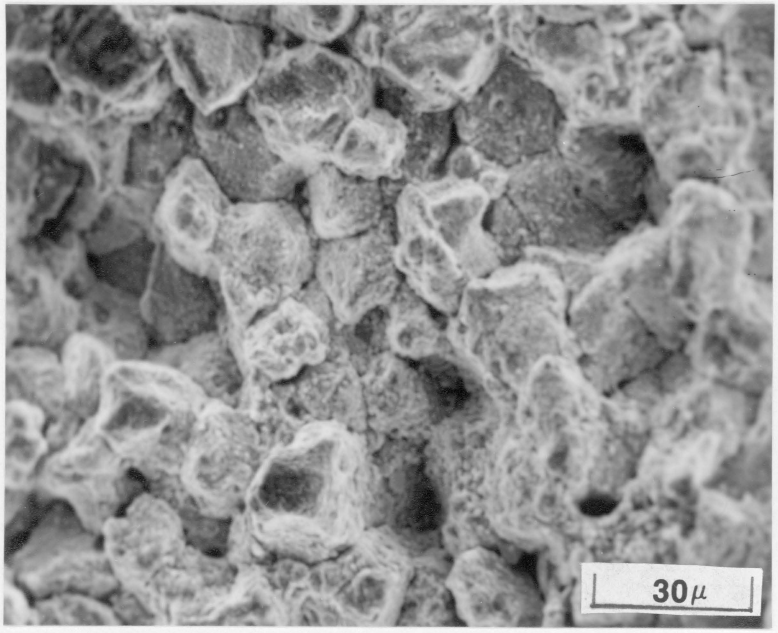

Figure 7. Fractograph of specimen 19 showing intergranular crack. Nature of the environmentally induced crack.

Table 3. Results from Slow Strain-Rate Tension Tests

Sample	D(in)	L(in)	a(in)	$\frac{L}{D}$	$\frac{(D-2a)L}{D^2}$	Percent Elongation to failure
12	.15	.75	.012	5	4.21	2.87
13	.15	.90	.010	6	5.20	2.80
14	.15	1.05	.007	7	6.39	4.35
15	.15	1.50	.008	10	8.96	2.50
16	.15	1.80	.010	12	10.40	1.81
18	.15	2.55	.009	17	14.93	1.80
19	.15	3.00	.009	20	17.53	1.60
21	.20	0.60	0.10	3	2.70	5.78
22	.20	1.00	.018	5	4.12	4.08
23	.20	1.20	.008	6	5.51	4.58
24	.20	1.40	0.12	7	6.16	2.89
31	.25	0.75	.010	3	2.76	5.80
32	.25	1.25	.010	5	4.59	4.49
33	.25	1.50	.006	6	5.69	4.00
34	.25	1.75	.010	7	6.43	2.46
35	.25	2.50	.007	10	9.41	2.34
36	.25	3.00	.008	12	11.26	1.85
37	.25	3.75	.011	15	13.64	1.82
39	.25	5.00	.010	20	18.38	1.56
42	.30	1.50	.011	5	4.63	3.95
43	.30	1.80	.008	6	5.68	4.08
44	.30	2.10	.006	7	6.70	4.41
45	.30	3.00	.009	10	9.41	2.19
48	.30	5.10	.018	17	14.99	1.92

*Conducted At A Constant Crosshead Displacement of $10^{-3}\frac{inch}{sec.}$

Table 4. Results From Slow Strain-Rate Tension Tests

Sample	Ultimate Tensile Strength (Ksi)	Strain-Rate ($\times 10^4$ sec^{-1})	Percent Reduction of Area	Length Of Test (Sec)
12	64.97	13.33	7.84	78
13	66.37	11.11	3.96	80
14	68.37	9.52	15.36	102
15	64.97	6.67	3.96	90
16	68.46	5.56	5.26	88
18	67.75	3.92	3.96	108
19	68.84	3.33	3.96	104
21	64.40	16.67	13.51	104
22	67.40	10.00	7.84	96
23	68.88	8.33	12.58	116
24	67.62	7.14	11.64	92
31	67.61	13.33	7.84	96
32	69.02	8.00	9.37	122
33	68.41	6.67	10.13	122
34	65.47	5.71	7.84	96
35	66.28	4.00	11.64	122
36	66.93	3.33	8.61	100
37	65.29	2.67	8.61	124
39	65.44	2.00	9.37	135
42	68.14	6.67	8.48	113
43	66.46	5.56	14.75	135
44	66.64	4.76	3.96	150
45	66.57	3.33	5.26	126
48	65.74	1.96	3.96	155

*Conducted At A Constant Crosshead Displacement of $10^{-3}\frac{inch}{sec}$

2 = 0.20 inch, 3 = 0.25 inch, and 4 = 0.30 inch. The second digit represented the relative $\frac{L}{D}$ ratio for the nine different cases.

Based on the results of Prabhat and Donovan [36] and the intuitive argument that increased crack instability would correlate to reduced percentage elongation to failure, engineering stress-percentage elongation curves were used to show the effect of the length to diameter, $(\frac{L}{D})$, ratio on crack instability. Curves for the nine different $\frac{L}{D}$ ratios are shown in Figures 8 through 16. The decrease in elongation to failure with increasing $\frac{L}{D}$ ratio is quite obvious. The data from Table 3 were determined from the computer printouts of these curves and accompanying hard data. Grip effects that are evident in Figures 8 through 14 were accounted for in the elongation to failure data. Crack lengths were estimated with optical microscopy.

With the visable trend of decreasing percent elongation with respect to increasing $\frac{L}{D}$ ratios, the trend should be better defined with respect to the effective $\frac{L}{D}$ ratio, $(D - 2a)\frac{L}{D^2} = (\frac{L}{D})_{eff}$. Figure 17 shows idealized results in the form of an engineering stress -elongation curve. To better define the trend between elongation and specimen dimensions, the elongation data in Table 3 were plotted as a function of $\frac{L}{D}$ and $(\frac{L}{D})_{eff}$ in Figures 18 and 19. Figure 19 clearly shows there is a well defined effect of specimen dimensions on elongation to failure data in slow strain-rate stress-corrosion cracking studies, based on the Paris analysis of elastic plastic tearing instability.

Statistical analysis of this data has shown that the elongation to failure in these studies is inversely proportional to $(\frac{L}{D})_{eff}$. A linear regression was performed to correlate the inverse of elongation to failure with $(\frac{L}{D})_{eff}$. The least squares fit was then evaluated using a t-statistic which measures the importance of a particular independent variable on a dependent variable [38]. The resulting data from this analysis showed that

$$\frac{1}{e} = (0.123 \pm 0.123) + (0.0301 \pm 0.00546)(\frac{L}{D})_{eff}$$

Where e is percent elongation to failure and the error intervals are stated ± twice the standard error (95% confidence). This regression accounted for 84.13 percent of data variance. As can be seen, these data fit a model with a zero constant term at 95% confidence. The t-statistic for the slope of the equation indicates a fit of the model with greater than 99.99 percent probability. Details of this and all other statistical analyses appear in Appendix B.

These results should alarm some investigators. The statement listed in ASTM specification G-49 that "axially loaded tension specimens provide one of the most versatile methods of performing a stress-corrosion test because of the flexibility permitted in the choice of type and size of test specimen....", is a statement that needs to be re-evaluated. The results of this investigation show that any SCC evaluation based on elongation to failure data must be done with consideration of the specimen dimensions. Figure 20 illustrates this point. Loss of elongation is a common way to characterize SCC susceptibility. Two specimens of different $(\frac{L}{D})_{eff}$ ratios would have different elongations to failure. This means results for a material-environment pair can not be directly compared if specimens are not the same dimensions. For that matter, different materials can not be compared directly for susceptibility to SCC in an environment unless they are properly sized to have the same $\frac{T_{app}}{T_{mat}}$ ratio. To evaluate a material strictly for SCC susceptibility, this ratio should be well below one so that unstable cracking due to the mechanical properties of the material does not occur. This same argument is applicable if work to failure (the area under the stress-elongation curve) is the parameter being used to evaluate SCC susceptibility. Since ultimate tensile strength is unaffected by the specimen dimensions (See Table 4), elongation would determine the work to failure. Time to failure (TTF) as a susceptibility parameter is also affected, since in a constant strain-rate test, it is a measure of elongation to failure.

Despite these results, not all parameters generally used to evaluate SCC appear to be affected by specimen dimensions. Both ultimate tensile strength and percent reduction of area appear to remain relatively constant with respect to the $\frac{L}{D}$ ratio. However, the elongation to failure dependence on specimen dimensions should make investigators wary of quantitatively ranking SCC susceptibility as some suggest [2, 9].

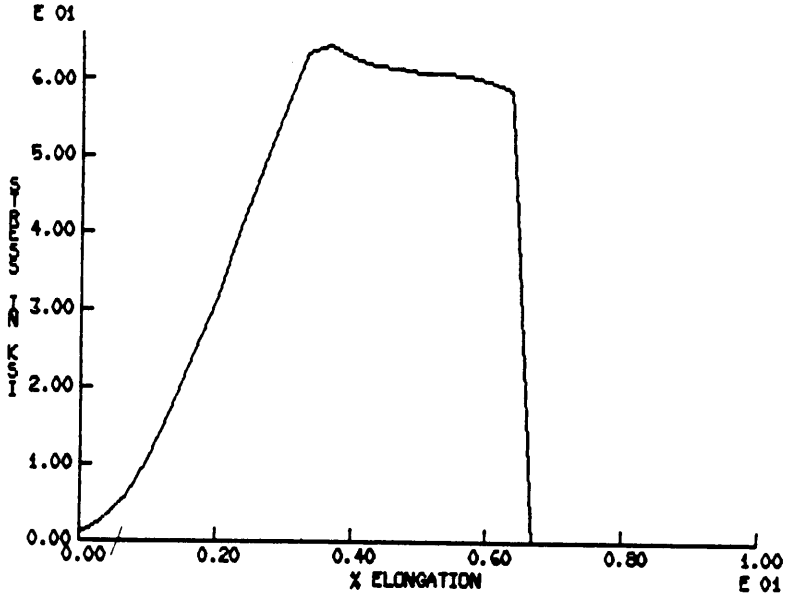

Figure 8. Engineering stress - percent elongation curve for specimen 21 ($\frac{L}{D}$ = 3) .

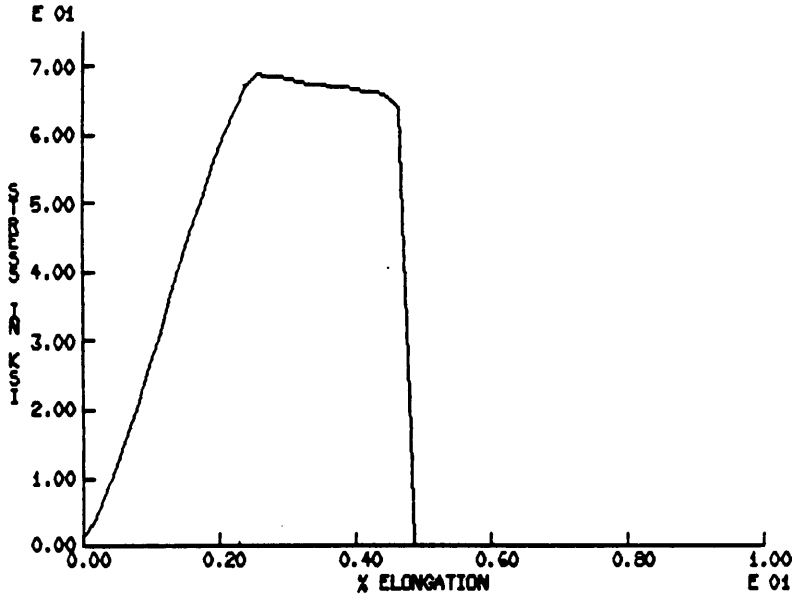

Figure 9. Engineering stress - percent elongation curve for specimen 32 ($\frac{L}{D} = 5$) .

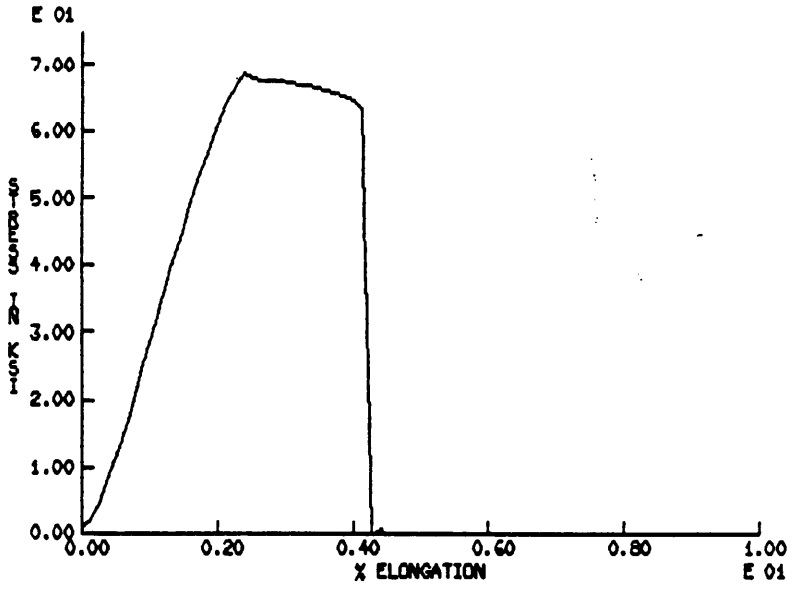

Figure 10. Engineering stress - percent elongation curve for specimen 33 ($\frac{L}{D} = 6$) .

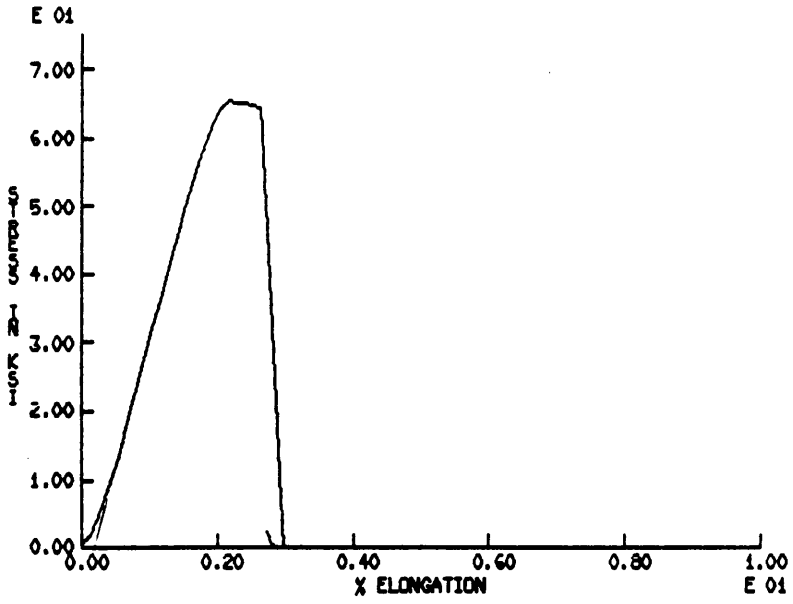

Figure 11. Engineering stress - percent elongation curve for specimen 34 ($\frac{L}{D} = 7$) .

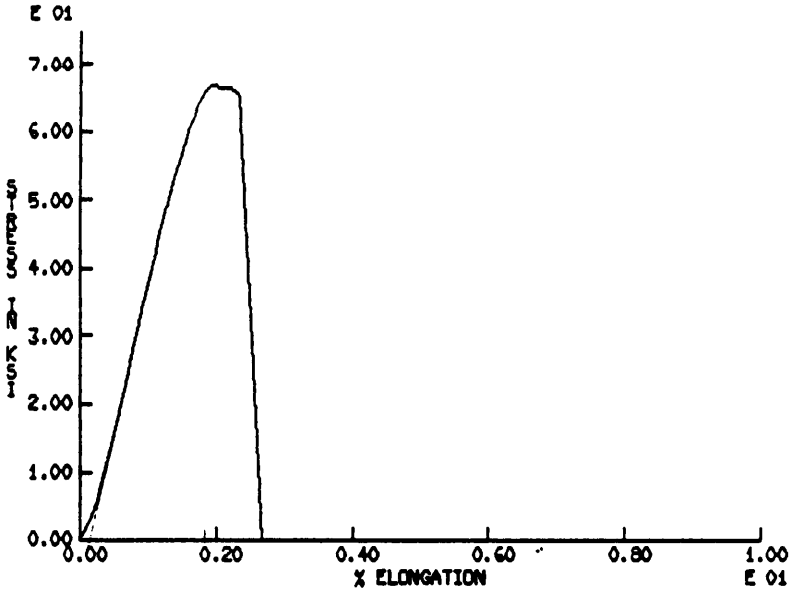

Figure 12. Engineering stress - percent elongation curve for specimen 45 $(\frac{L}{D} = 10)$.

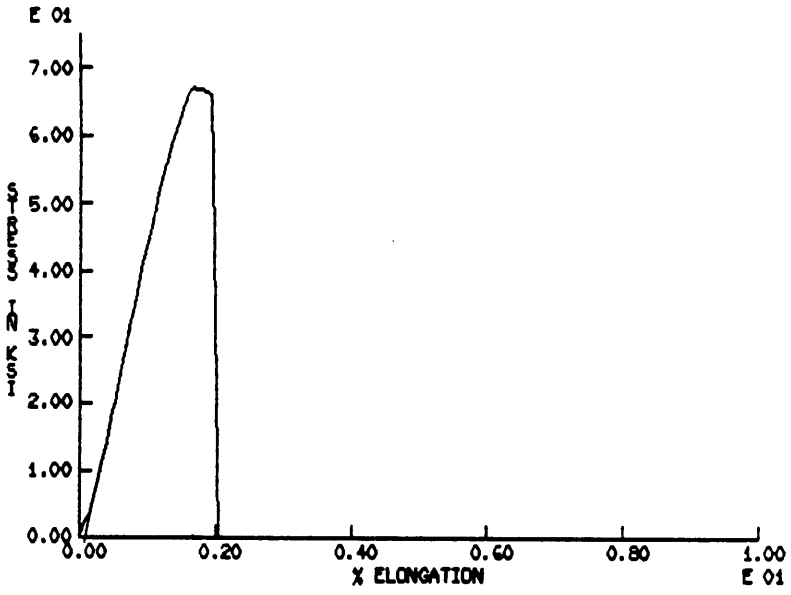

Figure 13. Engineering stress - percent elongation curve for specimen 36 ($\frac{L}{D}$ = 12) .

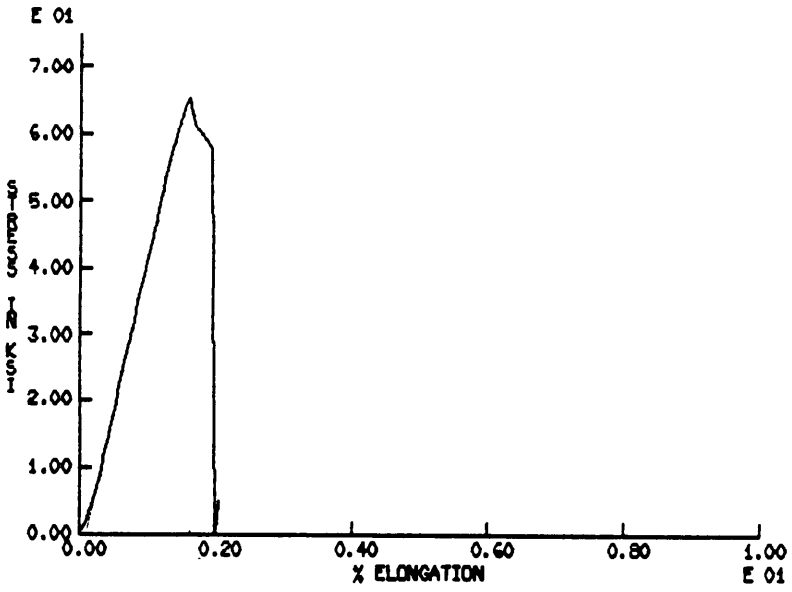

Figure 14. Engineering stress - percent elongation curve for specimen 37 ($\frac{L}{D}$ = 15) .

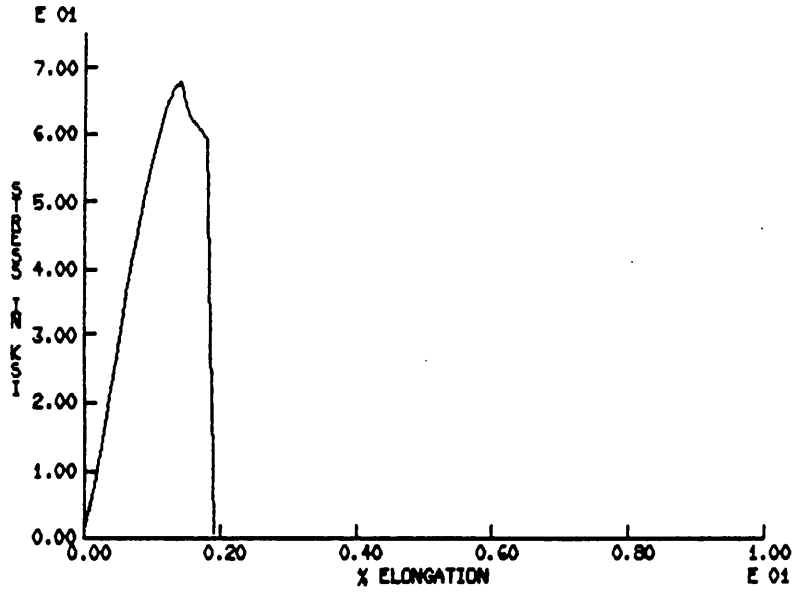

Figure 15. Engineering stress - percent elongation curve for specimen 18 ($\frac{L}{D} = 17$) .

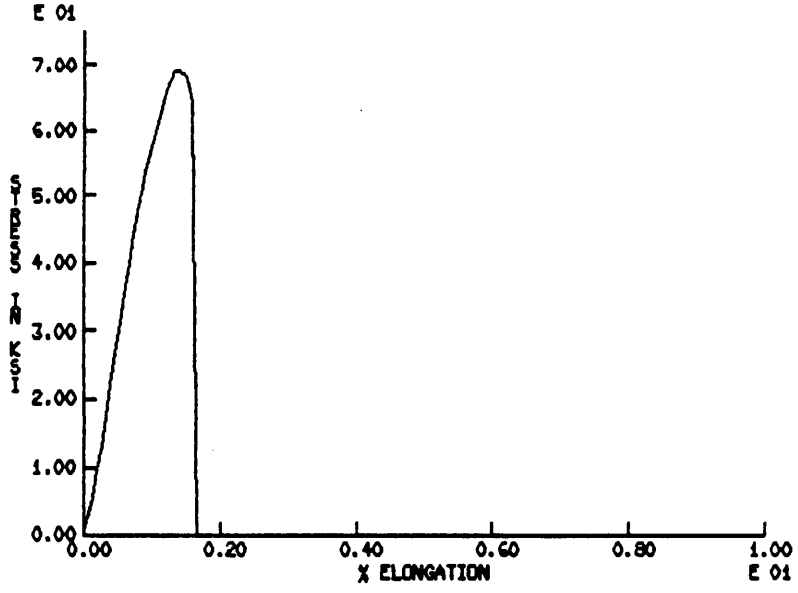

Figure 16. Engineering stress - percent elongation curve for specimen 19 ($\frac{L}{D} = 20$) .

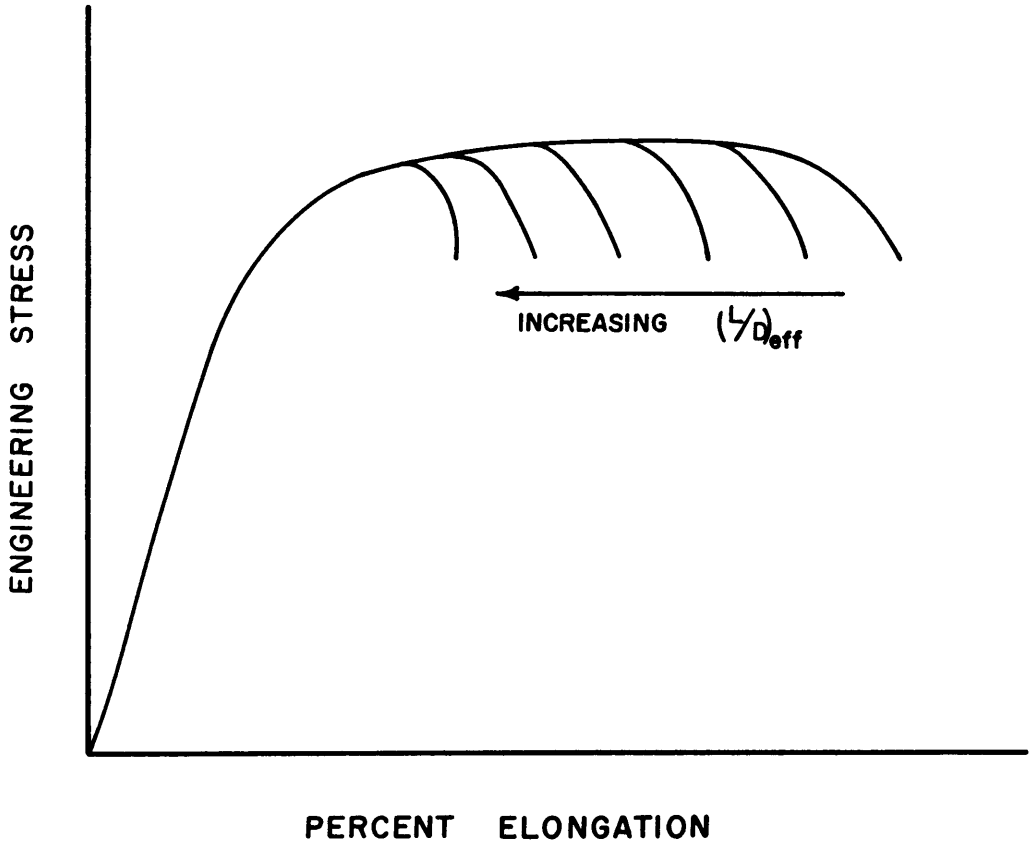

Figure 17. Idealized effect of increasing specimen dimensions. Elongation to failure decreases with increasing $(\frac{L}{D})_{eff}$.

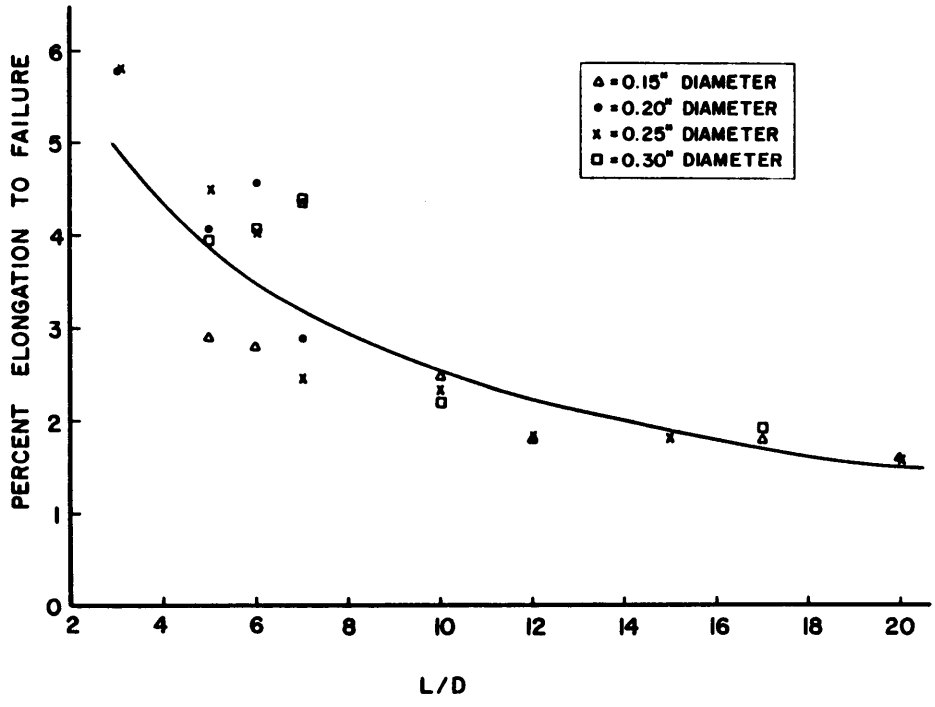

Figure 18. Percent elongation to failure plotted as a function of specimen dimensions. Curve fit using a reciprocal regression.

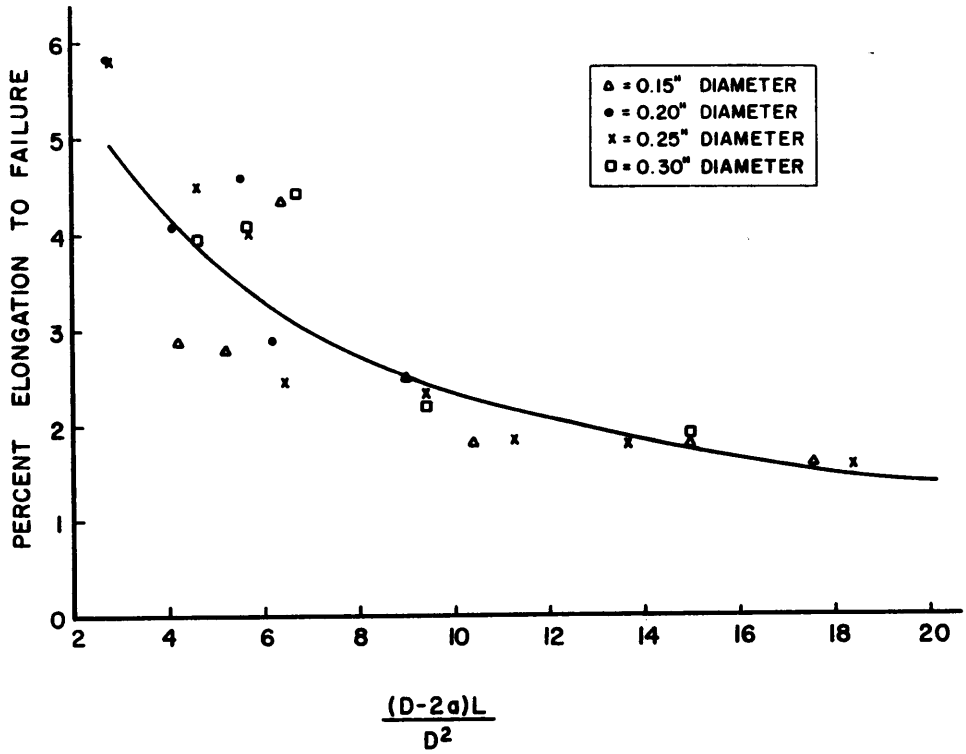

Figure 19. **Percent elongation to failure plotted as a function of T applied.** $\left(\frac{1}{4}T_{app} = \frac{(D-2a)L}{D^2} = \left(\frac{L}{D}\right)_{eff}\right)$ Curve fit using a reciprocal regression.

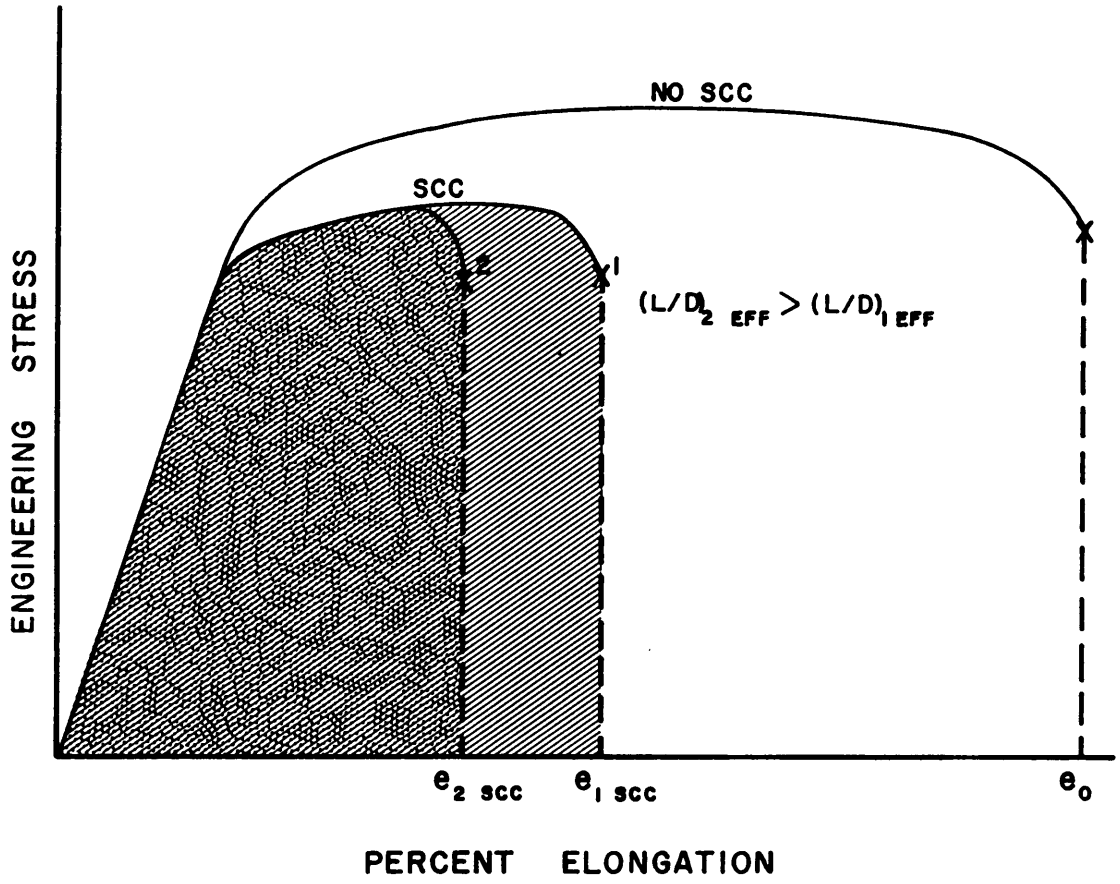

Figure 20. Effect of specimen dimensions on SCC evaluation. Engineering stress - elongation curve illustrating the possible effect of differences in specimen dimensions on measured SCC evaluation parameters.

4.3 *Discounting Strain-Rate Effects*

Initial examination of the data showed an apparent strain-rate effect in these tests. As shown in Figure 21, percent elongation to failure increased with strain-rate. Since the tests were conducted at constant crosshead displacement rate, based on the length of the reduced diameter portion of the specimen, the strain-rate varied inversely with length. The strain-rate effect that might be expected would be an increase in percent elongation with increasing strain-rate. At higher strain-rates there would be less time for environmental effects to occur and therefore the specimen would behave in a more ductile manner with a larger elongation to failure. Data from Tables 3 and 4 suggest this is the case and are plotted in Figure 21. There is an increase of elongation to failure with strain-rate. However, recall that there is an increase in elongation with decreasing $\frac{L}{D}$ ratio also. The large magnitude of the strain-rate effect is imaginary. This is just another indication of the specimen dimensions effect on elongation to failure.

Based on other observations, any large strain-rate effect can be disproved. Theoretically, at slower strain-rates, there would be more time for environmentally induced cracking and general embrittlement. Fracture would then be expected at a lower strain. Figures 22 and 23 show that this was not the case. Figure 22 shows that the environmentally induced crack length was relatively independent of strain rate. The data appears randomly scattered. The same is true for the relationship between time length of test and crack length plotted in Figure 23. Statistical analyses of these relationships confirms this conclusion. Using linear regressions as described before, crack length was correlated with strain-rate and time length of test independently. In both cases, the regression accounted for less than 1% of the data variance and the probability of any linear relationship modeling crack length as a function of either strain-rate or time length of test was less than 30%. Details of these regressions are in Appendix B. Additionally, microscopic evaluations shown in Figures 24 and and 25 confirm this conclusion. Two samples of the same $\frac{L}{D}$ ratio, but

tested at different strain rates and for different lengths of time, had similar patterns of secondary intergranular cracking.

These results show there was no large scale effect of strain-rate on the test results of this study. This is not to say there is no strain-rate effect. It is apparent in Figure 21 that four distinct lines can be drawn from the data for the different diameter sizes. Recall that each sample was prepared with the same surface area exposed to the degrading environment. Therefore, there were four different "effective" strain-rates. Once cracking began, deformation was limited to these exposed areas. The exposed section of the 0.15 inch diameter specimens was twice the length of the exposed section on the 0.30 inch diameter specimens. The lengths on the exposed sections of the other size diameter specimens fell in between these two. Therefore, the effective strain-rate after cracking began increased with diameter size. This explains the four different slopes based on diameter shown in Figure 21. Statistical analysis of normalized data verified this argument. To normalize the data in terms of the length of the exposed section, the percent elongation to failure was multiplied by the exposed length. The linear regression correlated this normalized value with test strain-rate. The resulting data from gave a constant of 0.307($\pm$.432) and a regression coefficient of 1030 ($\pm$ 116). The regression accounted for 78 percent of the data variance. This shows that the normalization reduced the data variance, therefore accounting for the exposed length differences. Details of the regression are given in Appendix B.

4.4 Implications

A slow strain-rate stress-corrosion cracking test does not represent many real life engineering situations, but is an indicator of possible stress-corrosion problems. Likewise this study has no direct impact on any specific engineering situations. However, it does suggest certain implications.

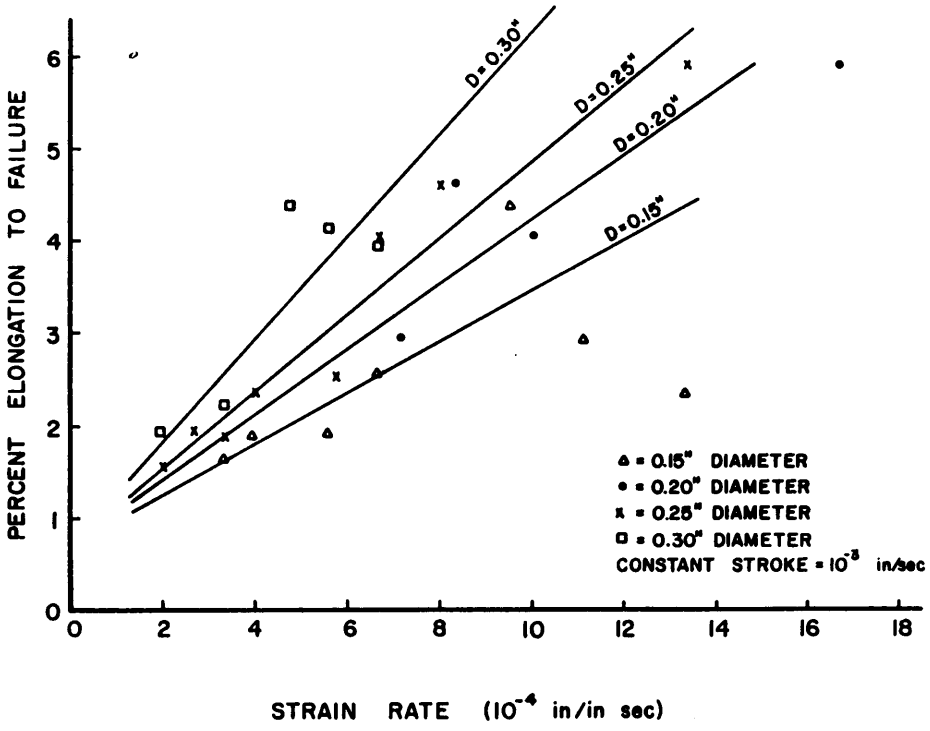

Figure 21. Percent elongation to failure as a function of strain-rate. The four different lines represent linear regressions of the data of the four different diameter sizes.

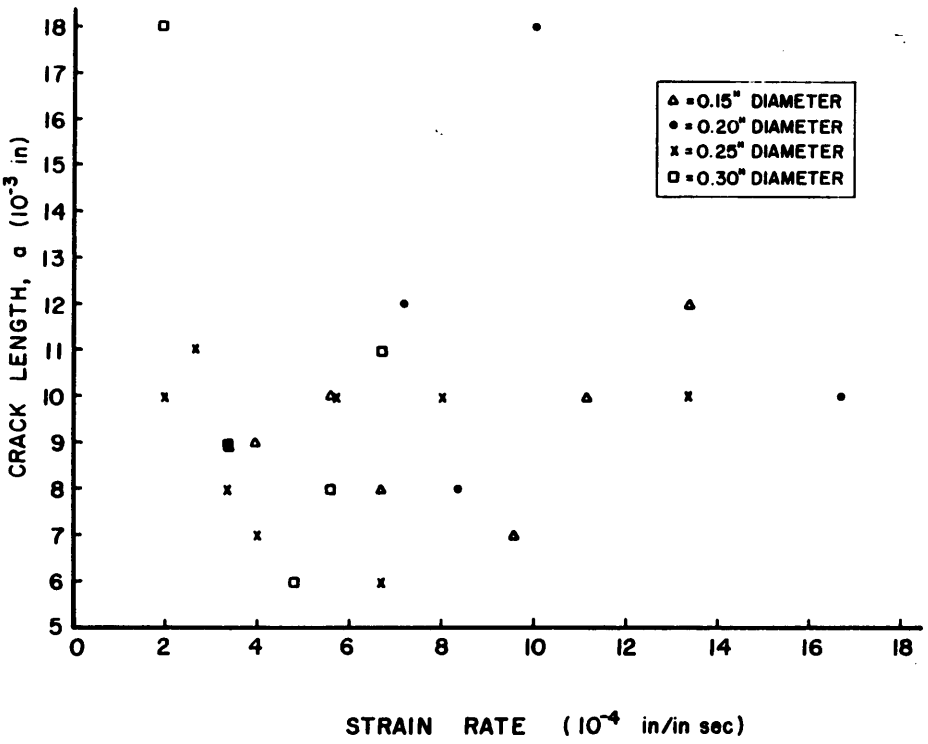

Figure 22. Plot of crack length as a function of strain-rate.

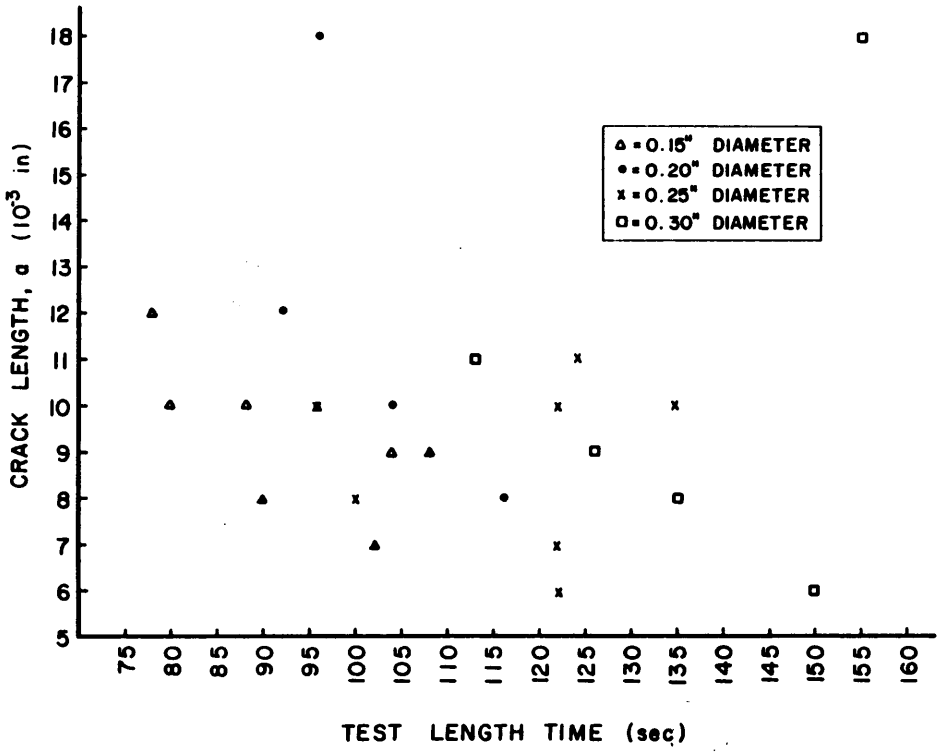

Figure 23. Plot of crack length as a function of time length of test.

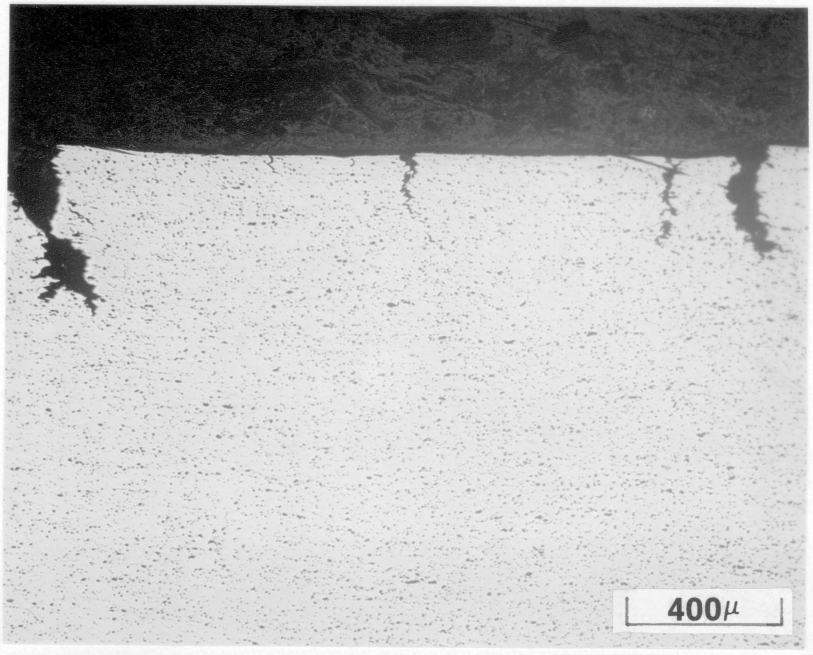

Figure 24. Micrograph of secondary environmental cracking in specimen 13. (D = 0.15 inch).

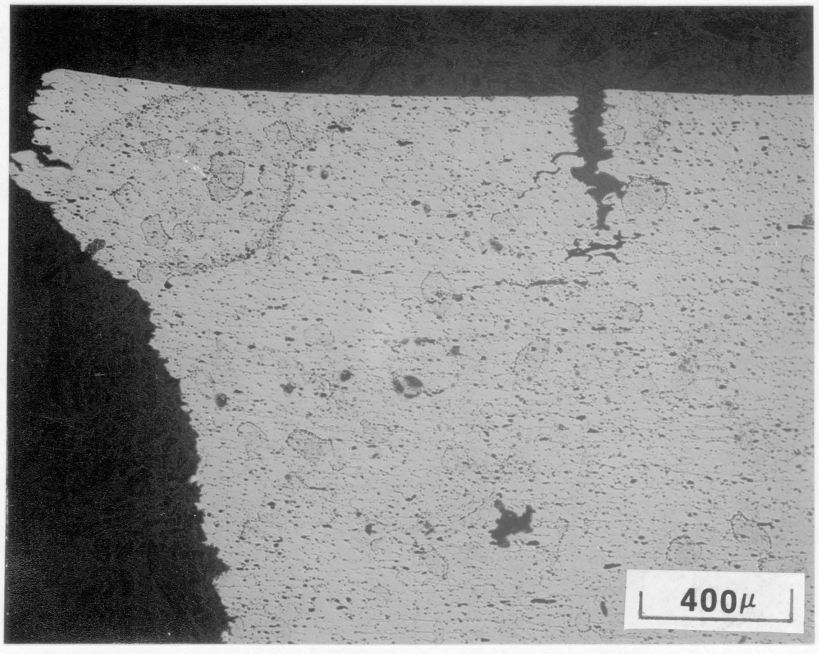

Figure 25. Micrograph of secondary environmental cracking in specimen 43. (D = 0.30 inch).

These results show that tearing instability should be a consideration in any materials selection process. This study was a critical experiment proving tearing instability can be predicted based on the Paris and co-workers work. Analysis for real engineering applications is feasible and should be applied. Such applications have been attempted by several investigators with reasonable success [32, 34, 35, 37].

The implications are more direct as related to the evaluation of SCC. The results show that improper evaluation of SCC data has probably occurred in the past. Almost all SCC studies involve microscopic verification of environmentally induced cracking, so it is doubtful that any materials have been incorrectly identifed for SCC susceptibility. However, the degree of susceptibility could have been misjudged. For example, consider a slow strain-rate SCC test program to determine material selection for a large scale application. If two different materials have distinctly different tearing moduli, similarly sized specimens will have distinctly different elongations to failure. If specimens are sized so that $T_{app} < T_{mat}$ for one material and $T_{app} > T_{mat}$ for the other, faulty analysis could occur. Material two could be less susceptible to SCC but have a smaller elongation to failure. Material one might then be selected for use based on this elongation data and later fail prematurely in service. In today's world, a mistake in materials selection such as this could involve a loss of millions of dollars.

5.0 Summary and Recommendations

5.1 Summary

In a study of the effects of specimen dimensions on results in slow strain-rate environmental effects tension testing, it was shown that the percent elongation to failure was inversely proportional to an effective length to diameter ratio, $\frac{(D - 2a)L}{D^2}$, in smooth round bar tensile specimens. This effective length to diameter ratio was, in essence, the applied tearing modulus as defined by Paris and co-workers in 1979. Thus, the results verify that the tearing modulus is a parameter which may be used to define tearing instability in terms of elastic-plastic fracture mechanics. These results also suggest possible inaccuracies in stress-corrosion cracking studies conducted with specimens that would undergo unstable ductile tearing once some critical fracture value is achieved. Possible strain-rate effects were shown not to exist.

5.2 *Recommendations*

A more detailed experimental analysis is required to determine how ductile tearing instability should be incorporated in slow-strain rate environmental testing. This would involve evaluating of the tearing moduli of several materials using $J - \Delta a$ data, and studying stress-corrosion susceptibility parameters in cases of stable and unstable mechanical crack growth. This would then be repeated for different specimen geometries, and variations from material to material would be compared. A comprehensive test procedure could then be determined.

The findings of this study show that there is a need for a tightly specified test procedure to evaluate environmental effects in materials using slow-strain-rate tensile testing techniques.

References

1. Payer, J.H., Berry, W.E., and Boyd, W.K., *Stress Corrossion - New Approaches*, ASTM STP 610, American Society for Testing and Materials, 1976, pp 82-93.

2. Payer, J.H., Berry, W.E., and Boyd, W.K., *Stress Corrosion Cracking - The Slow Strain-RAte Technique*, ASTM STP 665, American Society for Testing and Materials, 1979, pp 61-77.

3. Parkins, R.N., *Stress Corrosion Research*, Sijthoff and Noordoff International Publishers, The Netherlands, 1979, pp 1-28.

4. Parkins, R.N., *Stress Corrosion Cracking - The Slow Strain-Rate Technique*, ASTM STP 665, American Society for Testing and Materials, 1979, pp. 5-25.

5. Parkins, R.N., Mazza, F., Royuela, J.J., and Scully, J.C., *British Corrosion Journel*, Vol. 7, July, 1972, pp 154-167. Vol. 21, No. 6, 1981, pp 459-471.

6. Takano, M., Teramoto, K., and Nakayama, T., *Corrosion Science*, Vol 21, no. 6, 1981, pp. 459-471.

7. Kermani, M. and Scully, J.C., *Corrosion Science*, Vol. 19, 1979, pp. 89-110.

8. Vgiansky, G.M. and Johnson, C.E., *Stress Corrosion Cracking - The Slow Strain-Rate Technique*, ASTM STP 665, American Society for Testing and Materials, 1979, pp. 113-131.

9. Abe, S., Kojima, M., and Yuzo, H., *Stress Corrosion Cracking - The Slow Strain-Rate Technique*, ASTM STP 665, American Society for Testing and Materials, 1979, pp. 294-304.

10. Holroyd, N.J.H. and Scamans, G.M., *Environment - Sensitive Fracture: Evaluation and Comparison of Test Methods*, ASTM STP 821, American Society for Testing and Materials, 1984, pp. 202-241.

11. Frignani, A., Trabenelli, G., and Zucchi, F., *Corrosion Science*, Vol. 24, No. 11/12, 1984, pp. 917-927.

12. Stoltz, R.E., *Metallurgical Transactions A*, Vol. 12A, March 1981, pp. 543-545.

13. American Society for Testing and Materials, *Annual Book of ASTM Standards:*, Vol. 301, Designation: G49, pp. 284-291.

14. American Society for Testing Materials, *Annual Book of ASTM Standards*, Vol. 2.01, Designation: E8, pp. 1047-1067.

15. Treseder, R.S., *Laboratory Corrosion Tests and Standards*, ASTM STP 866, American Society for Testing and Materials, 1985, pp. 5-13.

16. Goods, S.H., *Metallurgical Transactions A*, Vol. 16A, June 1985, pp. 1031-1041.

17. Wei, R.P. and Novak, S.R., *Environment-Sensitive Fracture: Evaluation and Comparison of Test Methods*, ASTM STP 821, American Society for Testing and Materials, 1984, pp. 75-79.

18. Anderson, D.R. and Gudas, J.P., *Environment - Sensitive Fracture: Evaluation and Comparison of Test Methods*, ASTM STP 821, American Society for Testing and Materials, 1984, pp. 98-113.

19. Abramson, G., Evans, J.T., and Parkins, R.N., *Metallurgical Transactions A*, Vol. 16A, January 1985, pp. 101-108.

20. Yagawa, G., Takahashi, Y., and Ando, Y., *Engineering Fracture Mechanics*, Vol. 16, No. 5, 1982, pp. 721-731.

21. Rice, J.R., *Journel of Applied Mechanics*, Vol. 35, June 1968, pp. 379-386.

22. Landes, J.D. and Begley, J.A., *Fracture Analysis*, ASTM STP 560, American Society for Testing and Materials, 1974, pp. 170-186.

23. Landes, J.D. and Begley, J.A., *Fracture Toughness*, ASTM STP 514, American Society for Testing and Materials, 1972, pp. 24-39.

24. Rice, J.R., Paris, P.C., and Merkle, J.G., *Progress in Flow Growth and Fracture Toughness Testing*, ASTM STP 536, American Society for Testing Materials, 1973, pp. 231-245.

25. American Society for Testing and Materials, *Annual Book of ASTM Standards*, Vol. 3.01, Designation: E813, pp. 810-828.

26. Paris, P.C., Tada, H., Zahoor, A., and Ernst, H., *Elastic - Plastic Fracture*, ASTM STP 668, American Society for Testing and Materials, 1979, pp. 5-36.

27. Paris, P.C., Tada, H., Ernst, H., and Zahoor, A., *Elastic - Plastic Fracture*, ASTM STP 668, American Society for Testing and Materials, 1979, pp. 251-265.

28. Ernst, H.A., Paris, P.C., and Landes, J.D., *Fracture Mechancis: Thirteenth Conference*, ASTM STP 743, American Society for Testing and Materials, 1981, pp. 476-502.

29. Joyce, J.A. and Vassilaros, M.G., *Fracture Mechanics: Thirteenth Conference*, ASTM STP 743, American Society for Testing and Materials, 1981, pp. 525-542.

30. Vassilaros, M.G., Joyce, J.A., and Gudas, J.P., *Fracture Mechanics: Fourteenth Symposium*, Vol. 1, ASTM STP 791, American Society for Testing and Materials, 1983, pp. I65-I83.

31. McCabe, D.E. and Ernst, H.A., *Fracture Mechanics: Fourteenth Symposium*, Vol. 1, ASTM STP 791, American Society for Testing and Materials, 1983, pp. I561-I584.

32. Pan, J., Ahmad, J., Kanninen, M.F., and Popelar, C.H., *Fracture Mechanics: Fifteenth Symposium*, ASTM STP 833, American Society for Testing and Materials, 1984, pp. 721-745.

33. Zheng, C.Q. and Radon, J.C., *Advances in Fracture Research*, Vol. 2, Pergamon Press, New York, 1984, pp. 1197-1204.

34. Tada, H., Paris, P.C., and Gramble, R.M., *Fracture Mechanics: Twelfth Conference*, ASTM STP 700, American Society for Testing and Materials, 1980, pp. 296-313.

35. Kumar, V., German, M., and Shih, C.F., *Elastic-Plastic Fracture: Second Symposium*, Vol. 1, ASTM STP 803, American Society for Testing and Materials, 1983, pp. I306-I353.

36. Prabhat, K. and Donovan, J.A., *Environmental Degredation of Engineering Materials in Aggressive Environments*, VPI & SU, 1981, pp. 493-504.

37. Sciammarella, C.A., *Fracture Mechanics: Sixteenth Symposium*, ASTM STP 868, American Society for Testing and Materials, 1985, pp. 597-616.

38. Bowerman, B.L. and O'Connell, R.T., *Time Series and Forecasting: An Applied Approach*, PWS Publishers, Boston, 1979, pp. 61-62.

Appendix A. Test System Computer Program and Example Printout

A1. The program listed below was written using MTS BASIC Software to operate a MTS Model 810 servohydraulic test system. The program conducted the tensile test, recorded data, and output data in the forms of an engineering stress-percent elongation curve and a chart of recorded data.

```
100 REM   BILL'S TENSILE TEST PROGRAM (BLTENS.BAS) 9-APR-87
105 DIM A(250,2),M(250,2),K(250,2),X(1,1),N(1,1)
110 FGSTOP \ ADSTOP
111 CLRTXWIN
115 PRINT "THIS IS A TENSILE TEST PROGRAM THAT GIVES AN ENGINEERING STRESS"
120 PRINT "-ELONGATION DIAGRAM FROM CROSSHEAD DISPLACEMENT AND LOAD."
125 PRINT  \ PRINT "CURRENTLY THIS PROGRAM IS SET UP FOR ROD SPECIMENS."
140 PRINT  \ PRINT  \ PRINT "JUST FOR YOUR INFORMATION...."
145 PRINT  \ PRINT "FAILURE IS DEFINED BY A LOAD READING OF LESS THAN 2% FULL"
150 PRINT "SCALE AFTER LOAD HAS EXCEEDED 5% OF FULL SCALE."
155 PRINT  \ PRINT "A TABLE OF DATA AND A S-ELONGATION CURVE WILL HOPEFULLY BE"
160 PRINT "PRINTED AT THE END OF THE TEST."
165 PRINT  \ PRINT "ENTER THE FOLLOWING TEST PARAMETERS:"
170 PRINT  \ PRINT "SPECIMEN MATERIAL:"; \ INPUT M$
175 PRINT "DATE:"; \ INPUT D$
180 PRINT "YOUR NAME:"; \ INPUT B$
185 PRINT "TEST I.D. NAME: "; \ INPUT D1$
190 PRINT "SPECIMEN DIAMETER (IN):"; \ INPUT B1
195 PRINT "SPECIMEN LENGTH (IN):"; \ INPUT B2
200 PRINT "TIME TO FULL SCALE DISPLACEMENT (SECS):"; \ INPUT R
205 PRINT "STROKE RANGE SELECTED (IN):"; \ INPUT C
210 C1=C/R
215 PRINT "LOAD RANGE SELECTED (KIPS):"; \ INPUT D
220 IF R>0 THEN 230
225 PRINT "INVALID TIME!" \ GO TO 200
230 F=.25*PI*B1^2
235 PRINT  \ PRINT "LOAD SPECIMEN AND VERIFY CONTROLLER SETTINGS"
240 PRINT "ARE CORRECT.  VERIFY THAT STROKE AND LOAD ARE ZEROED."
245 PRINT  \ PRINT "BE VERY CAREFUL BEFORE YOU TURN ON HYDRAULICS"
250 PRINT "AND SWITCH TO LOCAL.  OUR MACHINE LACKS CERTAIN SAFETY"
255 PRINT "CONTROLS."
```

```
260 CLINIT
265 FGSTEP(1,0)
270 FGIMMED(1,"RAMP", TIME 1,0)
275 T=R
280 R1=R
285 IF T>2000 THEN 290
286 FGRAMP(1,T,1) \ GO TO 305
290 T=R-2000
295 T1=1-(T/R1) \ PRINT T1,T,R,R1
300 FGRAMP(1,2000,T1) \ R=T \ GO TO 285
305 REM HOPEFULLY THIS WORKS
310 ADLEVEL(1,A,,3,4.00000E-03,1)
315 ADRMAX(2,X,1) \ ADRMIN(3,N,1) \ REM CALLS TO DETECT ULT. LOAD AND FAILURE
320 ADTRIGGER(3,.05,1) \ REM STARTS FAILURE CHECK AFTER LOAD > 5% FULL SCALE
325 PRINT  \ PRINT "ENTER 'WE LOVE YOU BILL' TO START THE TEST"; \ INPUT Y$
330 IF Y$<>"WE LOVE YOU BILL" THEN 325
335 ADINIT \ ADGO \ FGGO
340 REM WAIT UNTILL FAILURE DETECT IS TRIGGERED
345 PRINT "OPERATING"
350 IF N(1,1)=0 THEN 350
355 REM ROUTINE TO MONITOR FOR FAILURE
360 IF ELEVEL(N(1,1))>.02 THEN 360
365 FGSTOP \ ADSTOP
370 FOR I=1 TO A
375 M(I,1)=(ELEVEL(A(I,1))-ELEVEL(A(1,1)))*100*C/B2
380 M(I,2)=ELEVEL(A(I,2))*D/F
385 NEXT I
390 FOR I=1 TO A
395 IF M(I,2)<.25 THEN 405
400 G=I \ GO TO 410
405 NEXT I
410 FOR I=G TO A
415 K(I,1)=M(I,1)-M(G,1)
420 K(I,2)=M(I,2)
425 NEXT I
430 TEKMODE
435 PHYL(1,0,100,0,100)
440 SCALE(1,0,0,10,0,75)
445 LABEL(1,'% ELONGATION','STRESS IN KSI',2,10,1)
450 AXES(1,0,0)
455 FOR I=1 TO A
460 PLOT(1,K(I,1),K(I,2))
465 NEXT I
470 COPY(1,1)
475 VTMODE(1,0)
480 PRINT  \ PRINT  \ PRINT
485 PRINT CHR$(27)+'[?5i'
490 PRINT  \ PRINT "OPERATOR'S NAME: ";B$
495 PRINT  \ PRINT "DATE: ";D$
500 PRINT "MATERIAL: ";M$
505 PRINT "TEST I.D. NAME: ";D1$
510 PRINT "SPECIMEN DIAMETER (IN): ";B1
515 PRINT "SPECIMEN LENGTH (IN): ";B2
520 PRINT "DISPLACEMENT RATE (IN/SECS): ";C1
521 PRINT "STRAIN RATE (IN/IN/SEC): ";C1/B2
525 PRINT "ULTIMATE LOAD (KIPS): ";ELEVEL(X(1,1))*D
530 PRINT  \ PRINT  \ PRINT  \ PRINT
535 PRINT "STRESS-ELONGATION DATA:" \ PRINT
540 PRINT ,"MEASURED DATA",,,"NORMALIZED DATA" \ PRINT  \ PRINT
545 PRINT ,"% ELONGATION","S (KSI)",,"% ELONGATION","S (KSI)"; \ PRINT
550 FOR I=1 TO A
555 PRINT I,M(I,1),M(I,2),,K(I,1),K(I,2)
560 NEXT I
565 PRINT CHR$(27)+'[?4i'
570 STOP
575 END
```

A2. The following is a sample output of results from the test system:

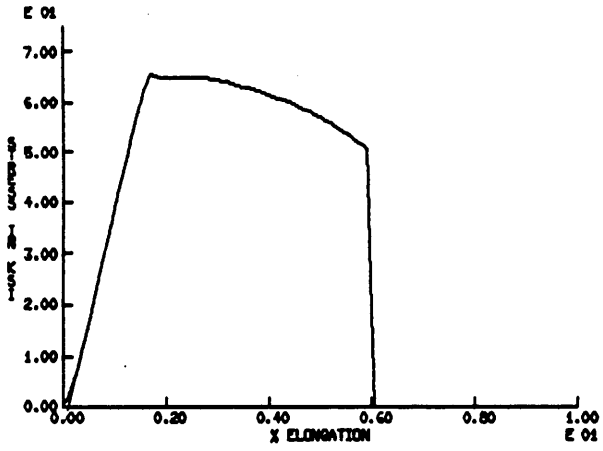

OPERATOR'S NAME: BILL

DATE: 7/29/87
MATERIAL: BRASS
TEST I.D. NAME: S-e 5
SPECIMEN DIAMETER (IN): .2
SPECIMEN LENGTH (IN): 2
DISPLACEMENT RATE (IN/SECS): 1.00000E-03
STRAIN RATE (IN/IN/SEC): 5.00000E-04
ULTIMATE LOAD (KIPS): 2.07303

STRESS-ELONGATION DATA:

	MEASURED DATA		NORMALIZED DATA	
	% ELONGATION	S (KSI)	% ELONGATION	S (KSI)
1	0	-.0894129	0	0
2	.100757	-.0699753	0	0
3	.201514	-.0311001	0	0
4	.299982	-.0699753	0	0
5	.399976	-.0777503	0	0
6	.499969	-.0699753	0	0
7	.599963	-.0699753	0	0
8	.699957	-.0660878	0	0
9	.799951	-.0738628	0	0
10	.900708	-.0505377	0	0
11	.999939	-.0622003	0	0
12	1.1007	-.0194376	0	0
13	1.20145	-.0855254	0	0
14	1.29992	-.0466502	0	0
15	1.39991	-.0388752	0	0
16	1.49991	-.0855254	0	0
17	1.5999	-.0777503	0	0
18	1.70219	-.0583128	0	0
19	1.80065	-.0660878	0	0
20	1.90065	-.0349877	0	0

21	1.99988	-.0311001	0	0
22	2.09987	.0272126	0	0
23	2.19987	.439289	0	.439289
24	2.29986	2.07593	.0999939	2.07593
25	2.39985	4.88661	.199988	4.88661
26	2.49985	8.3465	.299982	8.3465
27	2.59984	12.2612	.399976	12.2612
28	2.69984	16.3781	.499969	16.3781
29	2.79983	20.9226	.599963	20.9226
30	2.90364	25.2805	.703774	25.2805
31	2.99982	29.8561	.799951	29.8561
32	3.09981	34.4006	.899945	34.4006
33	3.1998	38.8868	.999939	38.8868
34	3.30056	43.4352	1.1007	43.4352
35	3.40056	47.7037	1.20069	47.7037
36	3.49979	51.9644	1.29992	51.9644
37	3.60054	55.9764	1.40068	55.9764
38	3.69977	59.7278	1.49991	59.7278
39	3.79977	63.1488	1.5999	63.1488
40	3.90053	65.5358	1.70066	65.5358
41	3.99976	65.0887	1.79989	65.0887
42	4.10051	64.8904	1.90065	64.8904
43	4.19974	64.8477	1.99988	64.8477
44	4.29974	64.9371	2.09987	64.9371
45	4.40049	64.941	2.20063	64.941
46	4.49973	64.9526	2.29986	64.9526
47	4.59972	64.9215	2.39985	64.9215
48	4.69971	64.9332	2.49985	64.9332
49	4.79971	64.8321	2.59984	64.8321
50	4.8997	64.7855	2.69984	64.7855
51	4.99969	64.665	2.79983	64.665
52	5.09969	64.56	2.89982	64.56
53	5.19968	64.3851	2.99982	64.3851
54	5.30044	64.1285	3.10057	64.1285
55	5.39967	63.9069	3.1998	63.9069
56	5.50119	63.6698	3.30133	63.6698
57	5.59966	63.4171	3.39979	63.4171
58	5.69965	63.1527	3.49979	63.1527
59	5.79965	62.8106	3.59978	62.8106
60	5.89964	62.4996	3.69977	62.4996
61	6.00116	62.2081	3.80129	62.2081
62	6.09963	61.8349	3.89976	61.8349
63	6.19962	61.4539	3.99976	61.4539
64	6.30038	61.0768	4.10051	61.0768
65	6.39961	60.6647	4.19974	60.6647
66	6.4996	60.2876	4.29974	60.2876
67	6.5996	59.8172	4.39973	59.8172
68	6.69959	59.3741	4.49973	59.3741
69	6.80035	58.927	4.60048	58.927
70	6.90034	58.4138	4.70048	58.4138
71	6.99957	57.8696	4.79971	57.8696
72	7.10033	57.3409	4.90046	57.3409
73	7.19956	56.7811	4.99969	56.7811
74	7.29955	56.1785	5.09969	56.1785
75	7.39955	55.6109	5.19968	55.6109
76	7.49954	54.9812	5.29968	54.9812
77	7.59954	54.2697	5.39967	54.2697
78	7.69953	53.6011	5.49966	53.6011
79	7.80029	52.8625	5.60042	52.8625
80	7.89952	52.1122	5.69965	52.1122
81	7.99951	51.3075	5.79965	51.3075
82	8.09951	50.4289	5.89964	50.4289
83	8.27201	-.136063	6.07215	-.136063

Appendix B. Statistical Analyses

In several instances during the evaluation of the results of this study, multiple regression statistical analyses were conducted to verify observed trends. These analyses were done using Anderson-Bell *ABstat*™ software, an interactive statistical package for the IBM PC.

In this study, linear regressions were performed on certain variable pairs to evaluate possible correlations between the two. A least squares curve of the form

$$y = \alpha + \beta x$$

was fit to the data, where y is the dependent variable, x is the independent variable, α is the estimated constant term, and β is the regression coefficient. The program then evaluates the fit of the curve using a t-statistic which measures the importance of a particular independent variable on a dependent variable [38]. The t-statistic is defined as

$$t = \frac{b}{s_b}$$

Where b is the least squares estimate of β and s_b is the standard error of the estimate b.

This number can be related to the probability that the linear model does not adequetly represent the data.

Regression printouts from the *ABstat*™ are shown for four data sets: the inverse of percent elongation to failure vs. $(\frac{L}{D})_{eff}$, crack length vs. strain rate, crack length vs. time length of test, and normalized percent elongation to failure vs. strain rate. The significant values in these printouts are: the coefficient of determination, which is the percentage of variation explained by the regression; the estimated constant term, α, and its standard error of estimate; the regression coefficient, β, and its standard error; and the t value, and the corresponding probability that the regression is not a true fit of the data. The F test, also printed, evaluates a model based on multiple independent variables. Since only one independent variable is used in each case, this value gives the same result as the t value. A rule of thumb for evaluating these regressions is that if |t| is greater than approximately 2, there is good statistical evidence that the two variables are dependent on one another.

B.1 The Inverse of Percent Elongation to Failure vs. $(\frac{L}{D})_{eff}$

*** MULTIPLE LINEAR REGRESSION ***

DEPENDENT VARIABLE: 13 ooe 24 VALID CASES

COEFF OF DETERM:	0.841345	ESTIMATED CONSTANT TERM:	0.122889
MULTIPLE CORR COEFF:	0.917249	STANDARD ERR OF ESTIMATE:	0.0617074

ANALYSIS OF VARIANCE FOR THE REGRESSION:

SOURCE OF VARIANCE	DEGREES OF FREEDOM	SUM OF SQUARES	MEAN OF SQUARES	F TEST	PROB
REGRESSION	1	0.444240	0.444240	116.666	0.0000
RESIDUALS	22	0.0837717	0.00380780		
TOTAL	23	0.528011			

VARIABLE	REGRESSION COEFFICIENT	STANDARDIZED COEFFICIENT	STANDARD ERROR	T	PROB
9 LDa	0.0300809	0.917249	0.00278497	10.8012	0.0000

B.2 Crack Length vs. Strain-Rate

*** MULTIPLE LINEAR REGRESSION ***

DEPENDENT VARIABLE: 4 a — 24 VALID CASES

COEFF OF DETERM: 0.00660738 — ESTIMATED CONSTANT TERM: 0.00944752
MULTIPLE CORR COEFF: 0.0812858 — STANDARD ERR OF ESTIMATE: 0.00305450

ANALYSIS OF VARIANCE FOR THE REGRESSION:

SOURCE OF VARIANCE	DEGREES OF FREEDOM	SUM OF SQUARES	MEAN OF SQUARES	F TEST	PROB
REGRESSION	1	1.36525E-006	1.36525E-006	0.146329	0.7057
RESIDUALS	22	2.05260E-004	9.32999E-006		
TOTAL	23	2.06625E-004			

VARIABLE	REGRESSION COEFFICIENT	STANDARDIZED COEFFICIENT	STANDARD ERROR	T	PROB
12 strate	0.627186	0.0812858	1.63957	0.382530	0.7057

B.3 Crack Length vs. Time Length of Test

*** MULTIPLE LINEAR REGRESSION ***

DEPENDENT VARIABLE: 4 a — 24 VALID CASES

COEFF OF DETERM: 0.00198460 — ESTIMATED CONSTANT TERM: 0.0105919
MULTIPLE CORR COEFF: 0.0445489 — STANDARD ERR OF ESTIMATE: 0.00306160

ANALYSIS OF VARIANCE FOR THE REGRESSION:

SOURCE OF VARIANCE	DEGREES OF FREEDOM	SUM OF SQUARES	MEAN OF SQUARES	F TEST	PROB
REGRESSION	1	4.10069E-007	4.10069E-007	0.0437481	0.8362
RESIDUALS	22	2.06215E-004	9.37341E-006		
TOTAL	23	2.06625E-004			

VARIABLE	REGRESSION COEFFICIENT	STANDARDIZED COEFFICIENT	STANDARD ERROR	T	PROB
6 test	-6.4833E-006	-0.0445489	3.09968E-005	-0.209160	0.8362

B.4 Normalized Percent Elongation to Failure vs. Strain-Rate

*** MULTIPLE LINEAR REGRESSION ***

DEPENDENT VARIABLE: 20 newel — 24 VALID CASES

COEFF OF DETERM: 0.780660 — ESTIMATED CONSTANT TERM: 0.306533
MULTIPLE CORR COEFF: 0.883549 — STANDARD ERR OF ESTIMATE: 0.216275

ANALYSIS OF VARIANCE FOR THE REGRESSION:

SOURCE OF VARIANCE	DEGREES OF FREEDOM	SUM OF SQUARES	MEAN OF SQUARES	F TEST	PROB
REGRESSION	1	3.66250	3.66250	78.3008	0.0000
RESIDUALS	22	1.02904	0.0467747		
TOTAL	23	4.69154			

VARIABLE	REGRESSION COEFFICIENT	STANDARDIZED COEFFICIENT	STANDARD ERROR	T	PROB
12 strate	1027.26	0.883549	116.090	8.84877	0.0000

The vita has been removed from the scanned document